International Journal of Steel Structures (2021) 21(4):1478–1501
https://doi.org/10.1007/s13296-021-00516-8

Online ISSN 2093-6311
Print ISSN 1598-2351

Reliability of Corroded Steel Members Subjected to Elastic Lateral Torsional Buckling

Ertugrul Turker Uzun[1] · **Engin Aktaş**[1]

Received: 12 June 2020 / Accepted: 9 July 2021 / Published online: 19 July 2021

Abstract
Structural steel members are subjected to corrosion due to environmental condition. As a result, there is decreasing in the cross-section properties of the member. This causes different stability problems and reduction in the load carrying capacity of members. Then, the probability of failure, P_f increases due to corrosion. The need arises to determine expected level of safety for such members and systems. Besides, reliability of the steel structure is also effected by the structural stability problems that result decreasing in the resistance. Lateral torsional buckling is one of the most encountered problems in steel members and affected by the critical moment which is a function of lateral and torsional stiffness. Critical moment depends on the material properties, boundary conditions, unbraced length, load pattern, and the member's cross section. Under the corrosion, it is inevitable to observe changing in some of properties. In this study, a damage model to determine the reliability of a corroded I-shape steel member under linear moment gradient is developed considering corrosion exposure time. Uniform and varying thickness loss models are considered to show the corrosion effect. Influence of environmental condition on the load carrying capacity of the members is considered and their effects on member design is evaluated. As a result, it is concluded that load carrying capacity of steel members degrades and safety of them adversely effected. With presented formulas, it is ensured that the load carrying capacity and reliability indices of the steel members can be calculated practically under the examined situations

Keywords Reliability · Corrosion · Lateral torsional buckling · I-shaped steel member · Moment gradient

1 Introduction

I-shaped steel members are widely used as a component of structures due to their capacity of bending and shear in the plane of the web. Although they present superior flexural rigidity in the major principal axis, the same is not necessarily true for the minor principal axis. I-beams subjected to bending about its major principle axis have an ordinary failure mode that is lateral torsional buckling. The behavior of members subjected to lateral torsional buckling changes from mainly in plane bending to combined lateral deflection, twisting, and finally failure pattern arises lateral deflection and twisting in combination with various extents of yielding and flange and/or web local buckling depending on the specific member characteristics unless properly braced against lateral deflection and/or torsion. On the other hand, lateral torsional buckling appears to be a complex problem depending on the various parameters, which are not well defined at the time of design (Ozbasaran et al., 2015). Thus, many different studies have been conducted to understand and design against the lateral torsional buckling. Some of the major studies on this issue come up with different approaches on beam buckling such as Kucukler et al. (2015), Valarinho et al. (2016), and Winkler et al. (2017). In order to reach more realistic results, finite element approaches and experimental studies were performed to assess lateral torsional buckling behavior of the members such as Aydin (2009), Jankowska-Sandberg and Kołodziej (2013), Wu and Mohareb (2013), Ghafoori and Motavalli (2015), and Yang et al. (2017).

Because of the observations and experiments that have been going on for years, corrosion has been shown to cause destructive and harmful effects on steel elements (Chandrasekaran & Nagavinothini, 2020; Kayser & Nowak, 1989). Detailed study is carried out to provide engineers with data

✉ Engin Aktaş
enginaktas@iyte.edu.tr

[1] Department of Civil Engineering, Faculty of Engineering, Izmir Institute of Technology, 35430 Urla, İzmir, Turkey

on thickness loss of structural steel members resulting from corrosion by Albrecth (2003). Especially, a reduction in fatigue life of corroded steel members are investigated experimentally considering numerous specimens taken from flanges and webs of corroded steel beams from steel bridges and petrochemical sites (Melchers, 1999; Rahgozar 1998; Sharifi & Rahgozar, 2009). The main effect of corrosion is the abrasions in the section size. This condition causes to decrease the structural load carrying capacity and structural safety to decrease (Sharif & Rahgozar, 2010; Sharifi & Rahgozar, 2010a). In order to predict service life and make reliable decision for deteriorating steel beams regarding the remaining moment capacity and shear failure, percentage thickness loss of the corrosion damaged I-beams are investigated (Sharifi & Rahgozar, 2010b, c). Due to thickness loss of flanges and web of the steel sections, section properties of members change and this cause stability problems like lateral torsional buckling (LTB) in the corroded steel beams (Melchers, 2003a; Rahgozar et al., 2010). In addition, there are difficulties in determining the reliability of structural performance due to uncertainties caused by the deterioration process caused by corrosion. Therefore, many studies from different perspectives have been carried out to overcome these uncertainties such as Melchers (2003a,b), Rahgozar (2009), Saydam and Frangapol (2011), and Sharifi and Tohidi (2014). Various factors such as environmental effects, load conditions, material properties etc. on corrosion resistance and behavior under lateral torsional buckling are investigated in detail by Chandrasekaran (2019), Chandrasekaran and Jain (2017), EN (1992), Timoshenko and Gere (1985).

In the light of all these developments, the study discusses the lateral torsion buckling of the I-shaped steel members and the corrosion effect on stability problem (LTB). Subsequently, the scope of this work is to demonstrate effect of corrosion induced deterioration impact on the reliability of the steel members. For this purpose, simply supported beams under linear moment gradient are investigated considering two different surface corrosion models that consist of uniform and varying thickness loss. Corrosion rates and probabilistic characterization have been determined by using available data from the literature. The reliability analysis is performed using these specified beams considering various exposure time and environmental conditions.

2 Resistance Model for Lateral Torsional Buckling (LTB)

In Fig. 1, a simply supported I shaped steel member is given. Constant end moments, M_o are applied at the end of the beam member. The differential equation representing

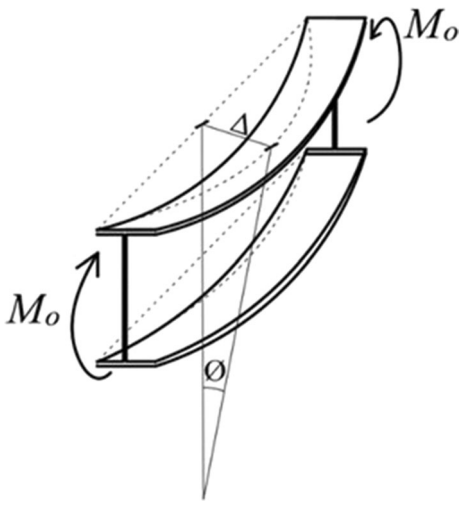

Fig. 1 Lateral torsional buckling of I-shaped member under uniform moment M_o

this condition is given in Eq. (1) by Timoshenko and Gere (1985).

$$\frac{d^4\emptyset}{dz^4} - \frac{GJ}{EC_w}\frac{d^2\emptyset}{dz^2} - \frac{M_0^2}{E^2 I_y C_w}\emptyset = 0 \tag{1}$$

where, E is the modulus of elasticity, G is the shear modulus, J is the polar moment of inertia, C_w is the warping constant, I_y is the moment of inertia with respect to the weak axis, and $\emptyset$ is the twisting angle.

The basic strength, M_{ocr} is the lateral torsional buckling resistance of a simply supported beam subjected to uniform bending moment along the unbraced length, L_b. It can be described as Eq. (2) and given by Timoshenko and Gere (1985) if boundary conditions are assumed as; both ends of the beam are not twisted but warped.

$$M_{ocr} = \frac{\pi}{L}\sqrt{EI_y GJ + \left(\frac{\pi E}{L}\right)^2 I_y C_w} \tag{2}$$

The maximum moment on the actual moment distribution can be represented by M_{cr}. Then, this is normalized by using a moment modification factor. This factor $C_b or\left(C_1 or \omega_2\right)$ can be developed to standardize M_{ocr} and M_{cr} values and it is given in Eq. (3);

$$C_b or\left(C_1 or \omega_2\right) = \frac{M_{cr}}{M_{ocr}} \tag{3}$$

The moment modification factor, C_b can be used to decide elastic lateral torsional buckling resistance of beam with multiplying the C_b by the basic strength, M_{ocr} of the member. All of the considered design standards and literature approaches express C_b, C_1, or ω_2 values as the moment modification factor.

According to design code procedures considered in this study, the nominal moment resistance of member subjected to elastic lateral torsional buckling can be calculated by using Eq. (4).

$$M_n = [C_b or(C_1 or \omega_2)] * M_{ocr} \tag{4}$$

In this study, EN 1993-1-1 (1992), BS5950 (2000), AS4100 (1998), AISC 360-16 (2016), TSDC-2016 (2016) and CSA-S16 (2014) standards are considered. Moreover, moment modification factor equations offered in the literature are used and a function based on the finite difference approach is proposed to calculate the critical moment capacity of the steel members under the effect of lateral torsional buckling.

EN 1993-1-1 (1992) defines the critical elastic lateral torsional buckling moment capacity for the case of beams with doubly symmetric sections in Eq. (5). In this equation, the member is assumed loaded from the shear center.

$$M_{cr} = C_1 \frac{\pi^2 E I_z}{(kL)^2} \left[\left(\frac{k}{k_w} \right)^2 \frac{I_w}{I_z} + \frac{(kL)^2 G I_t}{\pi^2 E I_z} \right]^{0.5} \tag{5}$$

where: I_t is the torsion constant, I_w is the warping constant, I_z is the second moment of area about the minor axis and L is the length of the beam between points which have lateral restraint. The effective length factors k and k_w vary from 0.5 for full fixity to 1.0 for no fixity, with 0.7 for one end fixed and one end free. For a case with k is equal to 1.0, the value of C_1 for any ratio of end moment loading is given with Eq. (6).

$$C_1 = 1.88 - 1.4\Psi + 0.52\Psi^2 \leq 2.70, \Psi = \frac{M_R}{M_L} \tag{6}$$

where: Ψ is the ratio of end moment loading.

British code, BS5950 (2000) offers an equivalent uniform moment factor with C_1 as a function of the maximum moment M_{max} and moments at the quarter points of the span M_A, M_B, and M_C in Eq. (7).

$$C_1 = \frac{M_{max}}{0.2M_{max} + 0.15M_A + 0.5M_B + 0.15M_C} \leq 2.273 \tag{7}$$

Australian steel design standard, AS4100 (1998) gives nominal moment capacity of member under elastic lateral torsional buckling with Eq. (8). AS 4100 specifies an additional factors α_m and α_s in Eqs. (9)–(10).

$$M_b = \alpha_m \alpha_s M_s \leq M_s \tag{8}$$

$$\alpha_m = \frac{1.7M_{max}}{\sqrt{\left[M_A^2 + M_B^2 + M_C^2\right]}} \leq 2.5 \tag{9}$$

$$\alpha_s = 0.6 \left[\sqrt{\left(\frac{M_s}{M_{oa}} \right)^2 + 3} \right] - \left(\frac{M_s}{M_{oa}} \right) \tag{10}$$

where, M_b is the nominal member moment capacity, M_s the nominal section moment capacity, M_{oa} is the reference buckling moment.

AISC 360-16 (2016) design specification has an approach which defines the critical elastic lateral torsional buckling for doubly symmetric sections with Eq. (11).

$$M_{cr} = C_b \frac{\pi}{L_b} \sqrt{EI_z GI_t + \left(\frac{\pi E}{L_b} \right)^2 I_z I_w} \tag{11}$$

where, L_b is the unbraced length of the beam member and C_b is the moment modification factor.

In addition to design standards and codes, the moment modification factor is studied and improved to represent capability of lateral torsional buckling behavior of members in literature. These factors are summarized below considering the appropriate literature works.

Moment modification factor, C_b is first studied by Salvadory (1955) with Eq. (12), Kirby and Nethercot (1979) presented an equation for C_b, which is applicable for any shape of moment diagrams. This equation is given in Eq. (13) and is accepted by AISC 360-16. Serna et al. (2006) proposed an alternative moment modification factor given in Eq. (14) using finite element techniques. Wong and Driver (2010) offered an equation given in Eq. (15) for moment modification factor by improving quarter-point formula.

$$C_b = 1.75 - 1.05\Psi + 0.3\Psi^2 \leq 2.3 \tag{12}$$

$$C_b = \frac{12.5M_{max}}{2.5M_{max} + 3M_A + 4M_B + 3M_C} \tag{13}$$

$$C_b = \sqrt{\frac{35M_{max}^2}{M_{max}^2 + 9M_A^2 + 16M_B^2 + 9M_C^2}} \tag{14}$$

$$C_b = \frac{4M_{max}}{\sqrt{M_{max}^2 + 4M_A^2 + 7M_B^2 + 4M_C^2}} \leq 2.5 \tag{15}$$

CSA-S16 (2014) use a similar approach specifies a factor ω_2, instead of C_b, which for nonlinear moment gradients. Expression of ω_2 in CSA-S16 is the same as that proposed by Wong and Driver.

TSDC-2016 (2016) has an approach for determining the lateral torsional buckling effects for the steel members and this approach is same to that of AISC 360-16 (2016). TSDC-2016 (2016) categorizes elastic and inelastic buckling considering unbraced length limits. Elastic lateral torsional

buckling may occur when unbraced length exceeds unbraced length limit, Eqs. (16)–(17) are used for calculating M_n.

$$M_n = F_{cr} W_{ex} \le M_p \tag{16}$$

$$F_{cr} = \frac{C_b \pi^2 E}{\left(\frac{L_b}{i_{ts}}\right)^2} \sqrt{1 + 0.078 \frac{Jc}{W_{ex} h_o} \left(\frac{L_b}{i_{ts}}\right)^2} \tag{17}$$

where: F_{cr} is the critical yielding point, W_{ex} is the elastic section modulus about the strong axis, J is the polar moment of inertia, h_o is the distance between the flange centroids and $i_{ts}^2 = \sqrt{I_y C_w}/W_{ex}$.

2.1 Finite Difference Approach for Lateral Torsional Buckling Calculation

A beam with unbraced length, L_b and subjected to uniform moment, M_o is considered in order to validate the finite difference approach to the solution of the fourth order differential equation of lateral torsional buckling in Eq. (1) by Uzun and Seçer (2019). The first term of the Taylor series of each derivative is used and the member is divided equal spaced grid points to obtain a numerical solution of $\emptyset$. Each of the length is Δz. Illustration of grid points used in finite difference approach is given in Fig. 2.

The derivatives of Ø (z) at the point $z = z_i$ can be described as Eqs. (18)–(21).

$$\emptyset_i' = \frac{1}{2\Delta z}\left(-\emptyset_{i-1} + \emptyset_{i+1}\right) \tag{18}$$

$$\emptyset_i'' = \frac{1}{\Delta z^2}\left(\emptyset_{i-1} - 2\emptyset_i + \emptyset_{i+1}\right) \tag{19}$$

$$\emptyset_i''' = \frac{1}{2\Delta z^3}\left(-\emptyset_{i-2} + 3\emptyset_{i-1} - 3\emptyset_{i+1} + \emptyset_{i+2}\right) \tag{20}$$

$$\emptyset_i'''' = \frac{1}{\Delta z^4}\left(\emptyset_{i-2} - 4\emptyset_{i-1} + 6\emptyset_i - 4\emptyset_{i+1} + \emptyset_{i+2}\right) \tag{21}$$

There are three constants determined by Eq. (22) and used to obtain finite difference description of differential equation at any arbitrary point i. Then, the equation becomes as Eq. (23).

$$a = \frac{EC_w}{\Delta z^4} b = -\frac{GJ}{\Delta z^2} c = -\frac{M_0^2}{EI_y} \tag{22}$$

$$a\left(\emptyset_{i-2} - 4\emptyset_{i-1} + 6\emptyset_i - 4\emptyset_{i+1} + \emptyset_{i+2}\right) + b\left(\emptyset_{i-1} - 2\emptyset_i + \emptyset_{i+1}\right) + c\emptyset_{i=0} \tag{23}$$

Suppose that the beam is divided into ten segments and Eq. (23) is calculated at grid points $i = 0, 1, 2, \ldots, 10$ so there are eleven equations. The boundary conditions at the two ends ($z = 0$ and $z = L$) are defined in Eq. (24).

$$\emptyset = 0 \Big|_{z=0,\ z=L} \quad \text{and} \quad \frac{d^2\emptyset}{dz^2} = 0 \Big|_{z=0,\ z=L} \tag{24}$$

Equation (24) can be written in the form as in Eq. (25) in the finite difference approximation. In here, the beam is divided into m segments.

$$\begin{matrix} \emptyset_i = 0 \\ \emptyset_{i-1} - 2\emptyset_i + \emptyset_{i+1} = 0 \end{matrix} \Bigg| \begin{matrix} z = 0 \rightarrow i = 0 \\ z = L \rightarrow i = m \end{matrix} \tag{25}$$

In this study, a member that is subjected to unequal end moments shown in Fig. 3 is investigated. M is chosen the larger absolute end moment and Ψ is accepted changing from − 1 to + 1 in order to consider possible cases of member end moments. The bending moment equation for the examined case is given in Eq. (26).

$$\mathrm{M_0} = \mathrm{M} - (1 + \Psi)\frac{\mathrm{M}}{\mathrm{L}}.\mathrm{z} \tag{26}$$

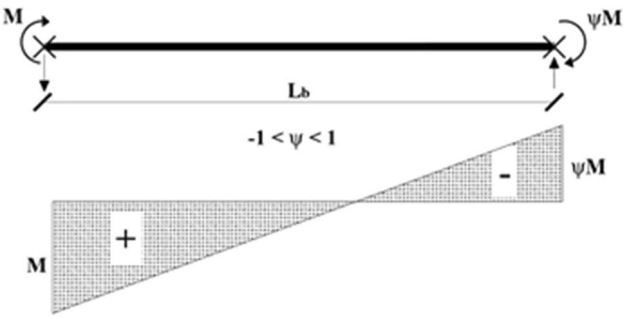

Fig. 3 Bending moment diagram in a member subjected to unequal end moments

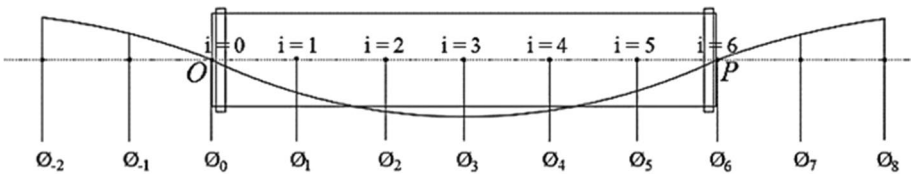

Fig. 2 Example of grid points in finite difference approximation

Equation (26) can be described as Eq. (27) for finite difference approach.

$$M_0 = M\left[1 - (1+\Psi)\frac{i}{L}\cdot\Delta z\right] \tag{27}$$

By substituting moment, M_0 in Eq. (27) into Eq. (1), the differential equation used in the finite difference approach for investigated load case becomes as Eq. (28).

$$\frac{d^4\emptyset}{dz^4} - \frac{GJ}{EC_w}\frac{d^2\emptyset}{dz^2} - \frac{M^2}{E^2 I_y C_w}\left[1-(1+\Psi)\frac{i}{m}\right]^2\emptyset = 0 \tag{28}$$

Finite difference calculation procedure is used for calculating the differential equation in Eq. (28). In the analyses, the member is considered divided into 300 elements. In order to satisfy accuracy of analysis results, MATLAB (2018a) software is used. Afterward, critical moment values caused lateral torsional buckling in the member is determined. Moment modification factor value, C_b that is used to adjust the lateral torsional buckling equations is presented for each moment gradient value. Outcomes from the finite difference analysis are given in Fig. 4.

The relationship between moment modification factor, C_b and Ψ values of the end moments are generated using analysis results and given in Eq. (29).

$$C_b = \frac{-1.63\Psi + 3.69}{\Psi^2 - 2.27\Psi + 2.03} \tag{29}$$

2.2 Finite Element Buckling Analysis

Finite element based software can be useful in order to determine the load carrying capacity of members. They have high processing capacities in the analyses. Moreover, geometric and material nonlinearities in the analyses steps can be induced by them. Therefore, ANSYS (2015) software is used to analyze I-shaped steel members. Model is considered as symmetric. The web and both flanges of steel member are modelled using four side shell elements SHELL 43 from the ANSYS element library. Mesh sizes are generated about 40 × 40 mm.

Translations u_x, u_y, u_z and rotations $\varphi_x, \varphi_y, \varphi_z$ are related to global coordinate system. Boundary conditions of both end of the beam examples are modeled as $u_y = u_z = \varphi_x = 0$. This condition is illustrated in Fig. 5.

2.3 Validation of Proposed Method

A laterally unrestrained steel beam IPE500 subjected to the static bending moment around its major axis is selected for validation of the proposed method and shown in Fig. 6.

In order to investigate the structural behavior and the efficiency of the proposed formula, various end moment ratios $-1 < \Psi < 1$ are considered in the present study. Moreover, design code procedures for EN 1993-1-1 (1992), BS5950 (2000), AS4100 (1998), AISC 360-16 (2016), TSDC-2016 (2016) and CSA-S16 (2014) and recommended moment modification factor equations by the researchers such as Salvadory (1955), Serna et al. (2006), Wong and Driver (2010) are considered in the analyses. Outcomes of proposed and other methods are compared with each other.

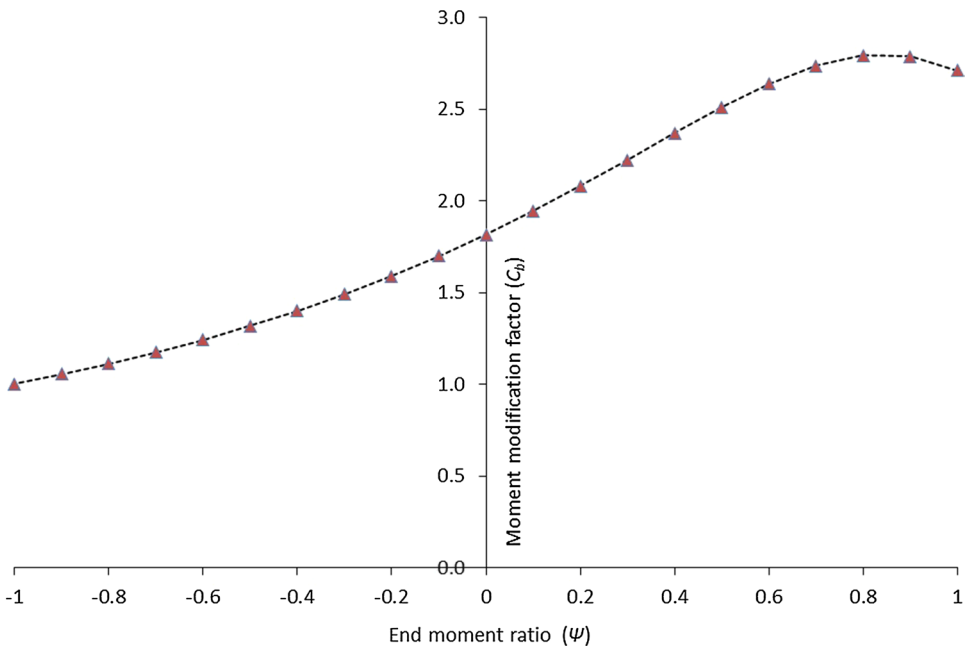

Fig. 4 Moment modification factors, C_b for a beam subjected to unequal end moments, Ψ

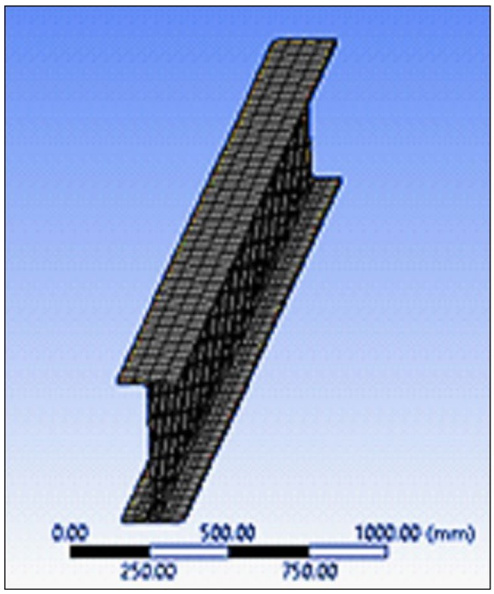

Fig. 5 FEM model of the beam members and boundary conditions

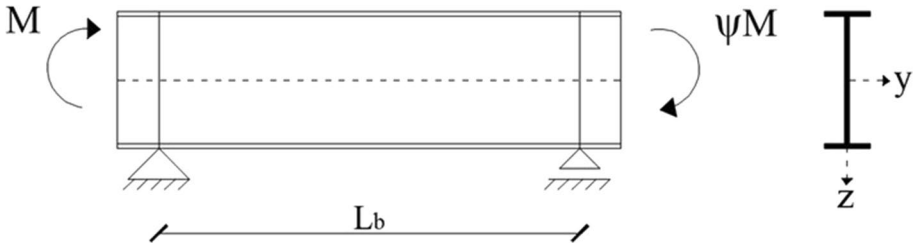

Fig. 6 Simply supported beam under linear moment gradient

In order to carry out the comparison of results, the curves are plotted in Figs. 7, 8. These curves include moment capacities standardized by dividing M_{cr} by the theoretical elastic buckling strength, M_{ocr} in horizontal axes and the various end moment ratios, Ψ in vertical axes.

Calculated moment modification factor values (M_{cr} / M_{ocr}) indicate that, AS4100 are relatively low when compared to other design code and literature approach results. Therefore, AS4100 gives more conservative results than the other approaches. In addition, BS5950 gives approximately same results with AISC360-16 and CSA-S16. EN 1993-1-1 gives very close values with results of FEM and the proposed method equation.

3 Corrosion Effect

The effects of corrosion on metals have been studied by researchers for many years through studies conducted in various environments. From data comes from these studies showed that corrosion loss follow an exponential function given in Eq. (30) (Komp, 1987).

$$C = At^B \tag{30}$$

where: C represents the average corrosion penetration (μm), t is the number of years, A and B are the parameters determined from the analysis of experimental data. In Table 1, A and B values are given.

In order to show deterioration effect of corrosion on the steel members, corrosion penetration versus time graphic is plotted and given in Fig. 9.

3.1 Corrosion Loss Model

Corrosion model is required the information about the location where the corrosion occurs and the types of corrosion. There are five main forms of corrosion, which can affect a steel girder (Albrecht & Hall, 2003). The most common form of corrosion caused damage in the steel members is surface corrosion. This form leads to the gradual destruction and thinning of members (Fontana, 1987).

Two different corrosion models have been emphasized in the literature. These are uniform and varying thickness loss models. Uniform thickness loss model is applied to whole section of the model. However, actual corrosion damage is

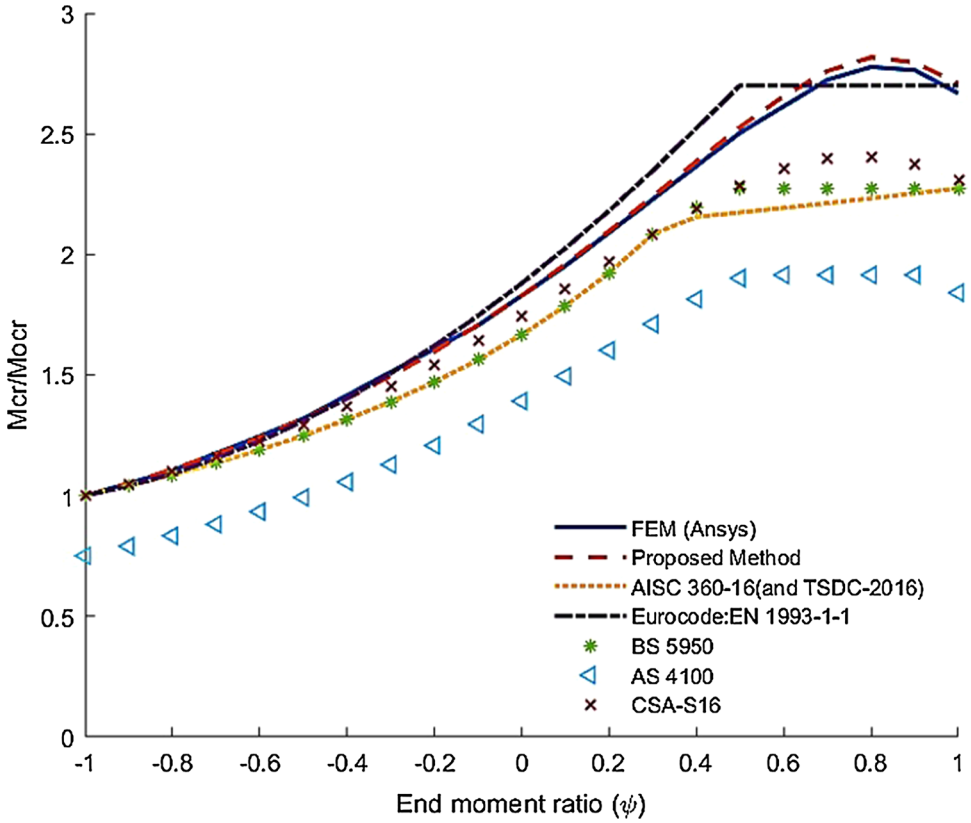

Fig. 7 End moment ratio (Ψ) versus M_{cr}/M_{ocr} considered design codes

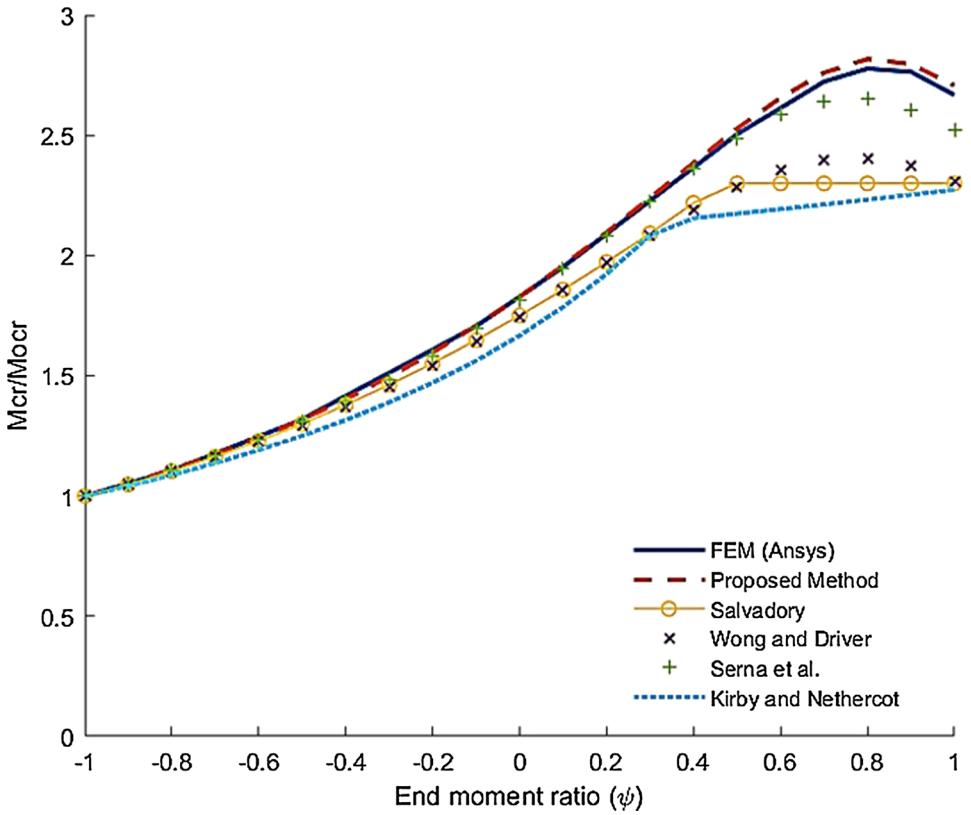

Fig. 8 End moment ratio (Ψ) versus M_{cr}/M_{ocr} considered literature work

Table 1 Average values for corrosion parameters *A* and *B* for carbon and weathering steel (Kayser & Nowak, 1989)

Environment	Carbon steel		Weathering steel	
	A	B	A	B
Rural	34.0	0.65	33.3	0.5
Urban	80.2	0.59	50.7	0.57
Marine	70.6	0.79	40.2	0.56

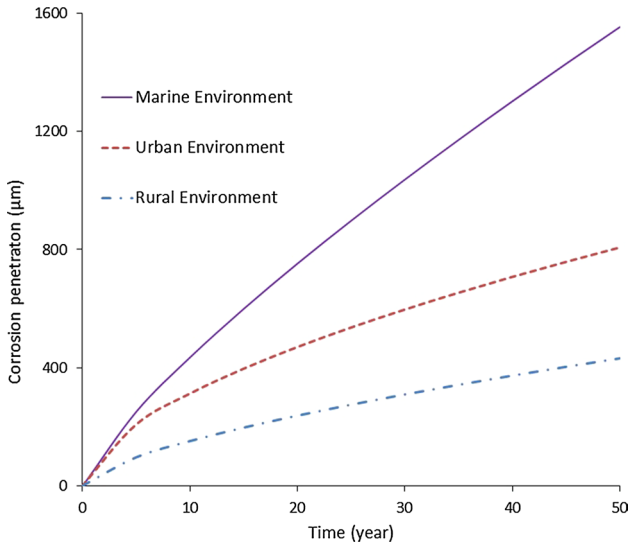

Fig. 9 Corrosion penetration versus time (year) for carbon steel considering different environment

locally and not uniform. Therefore, it would be more accurate to use varying thickness loss model. In this way, results that are more realistic can be achieved.

Since the two models have been examined in the literature, both of them are investigated in the study and the results are given for comparison. For this purpose, the corrosion decay model developed by Rahgozar (2009) for uniform and varying thickness loss model sections are considered and given in Figs. 10 and 11.

After a structural steel member is exposed to, the corrosion for a certain time, basic changes in the member is expected. Material loss and reduction in the section property are the most important problems encountered. A reduction in the cross-section values of the member is one of the topics that this study examines because the important geometric properties (moment of inertia, torsion constant, warping constant etc.) of section are changed. In addition, buckling capacity of members is expected to decrease dramatically due to these changes.

IPE section type steel elements, which are commonly used, have been chosen in order to investigate and determine the capacity reduction of I-shaped steel elements due to corrosion. Selected IPE sections and their properties are given in Table 2.

Remaning capacity (RC) of different IPE shape steel members are investigated considering corrosion loss models for various environment conditions. The moment capacities of the sections are taken as the basis in the analyses and losses of the web thickness are considered. Results are given in Figs. 12, 13, 14 for uniform thickness loss model and Figs. 15, 16, 17 for varying thickness loss model.

According to analysis results, it is observed that % RC for IPE section beams dramatically decrease depend on the environmental conditions and the years of corrosion exposure. Ultimate reductions in capacity based on 50 years are given in the Table 3 for uniform thickness loss and Table 4 for varying thickness loss model.

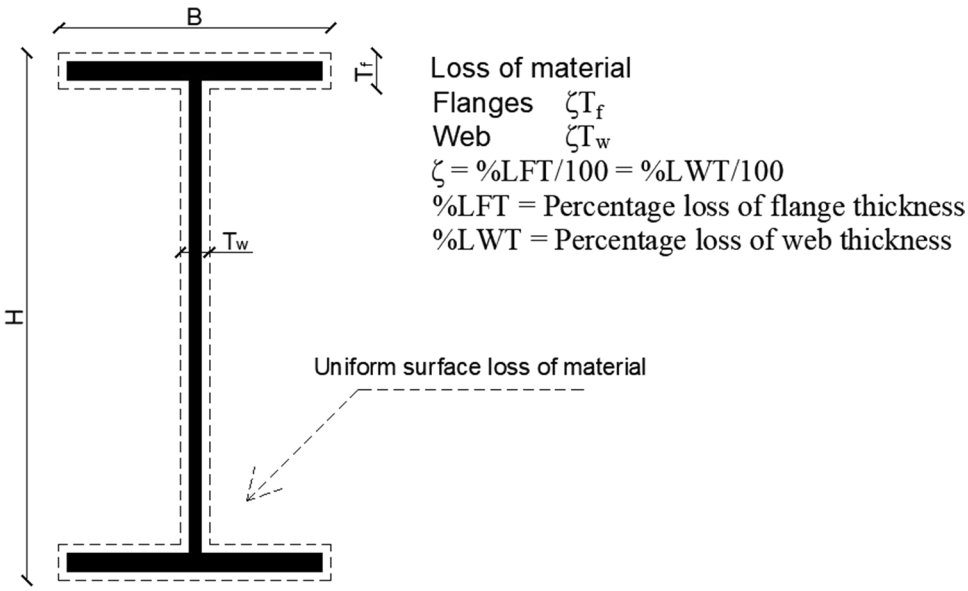

Fig. 10 Corrosion loss model for uniform thickness loss

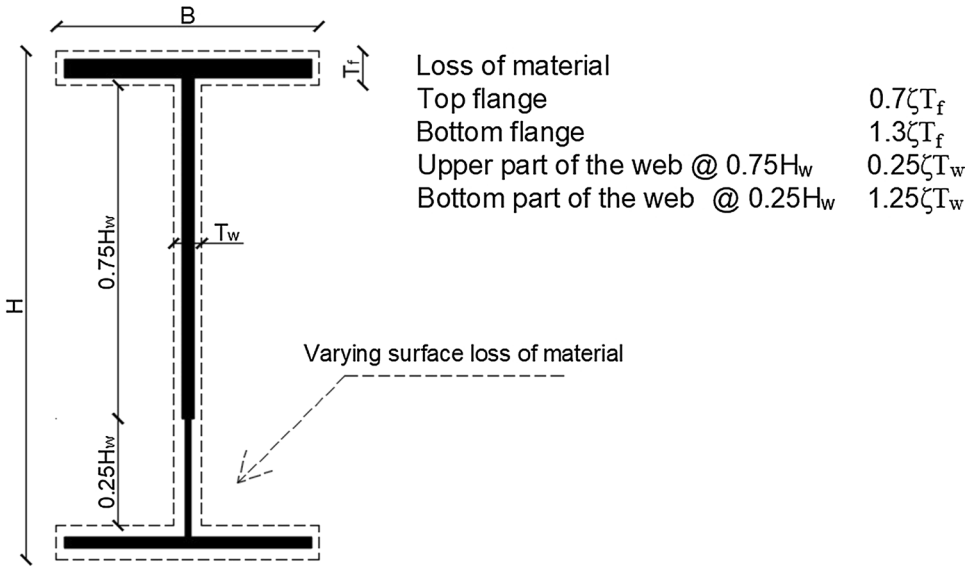

Fig. 11 Corrosion loss model for varying thickness loss

Table 2 IPE section properties

Section type	Dimensions (mm)			
	H	B	T_f	T_w
IPE500	500	200	16	10.2
IPE400	400	180	13.5	8.6
IPE300	300	150	10.7	7.1
IPE200	200	100	8.5	5.6
IPE100	100	55	5.7	4.1

The ultimate capacity decrease of all sections (except IPE500) at the end of 50 years corrosion exposure are compared with the ultimate capacity decrease of IPE500 in 50 years. Results are illustrated in Figs. 12, 13, 14, 15, 16, 17 as % Difference. According to this, ultimate capacity reduction becomes higher as the cross-section properties of the I-shaped beams decrease. Moreover, it can be concluded that I-shaped steel beams, which have smaller cross-section properties, are suffered more by corrosion.

The thickness loss in the flanges and web due to corrosion, results in reduction in the moment capacity of the member. Besides this, the loss of thickness may change the class of an element (plastic, compact, semi-compact or slender) from one to another. However, all sections are examined accordingly and not all of the sections exposed to corrosion for 50 years show change in their class. Despite very close limit values for IPE100 and IPE200, the desired range has been maintained. In addition, the reduction in moment capacity is linearly proportional to the flange thickness loss like the web thickness loss of the members.

Varying thickness loss model cause to locally and not uniform damage. However, uniform thickness loss model cause uniform damage in the section due to corrosion. Therefore, capacity decreasing in the sections reaches very high levels for uniform section loss model.

In addition, changes in capacity depending on the corrosion environment and time exposure can give an idea to the designer when building an engineering structure that is prone more to damage due to corrosion.

4 Reliability Analysis of I-Shaped Steel Beams

The strength, R of a structural member that is referred resistance and the load effect, Q cannot be precisely determined so they are both random variables. The probabilistic description of strength and load effect is given in Fig. 18.

If $Q \leq R$, structural behavior is satisfactory. However, $Q > R$ is undesirable. The reliability of a structure or structural component corresponds to its ability to safely withstand the imposed actions and fulfill requirements of serviceability and durability. The aim of using probabilistic methods is determining the probability of failure and reliability index, β. In Fig. 19, identical representation of probabilistic description is given.

Since the probabilistic distributions of R and Q are not known exactly, First-Order Second-Moment (FOSM) reliability method has been used to operate only mean and standard deviation of the random variables (Ellingwood et al., 1980). According to the first-order probabilistic method, reliability index, β can be determined using Eq. (31) if the resistance and the load effect are assumed to distribute lognormally.

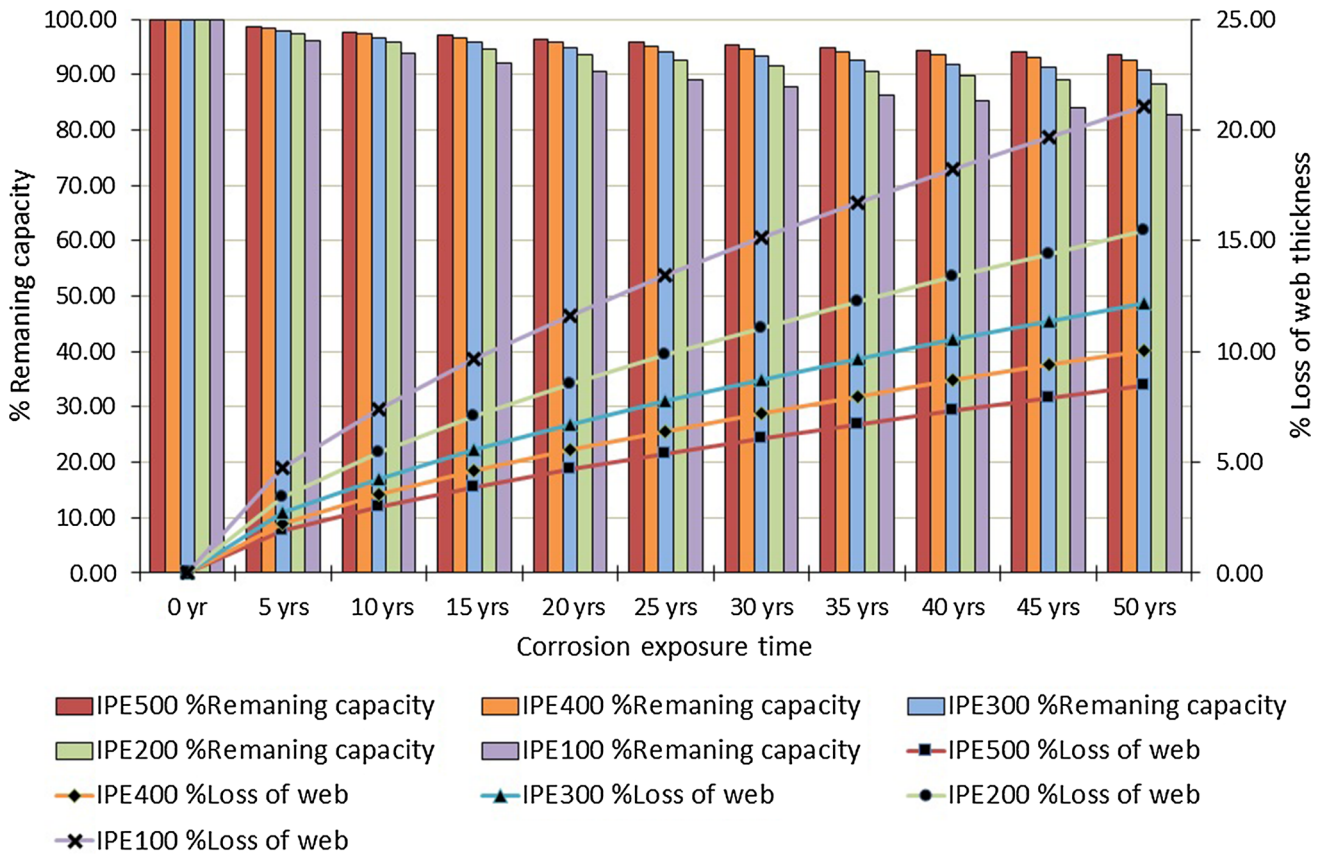

Fig. 12 % Remaining capacity versus % Loss of web thickness due to corrosion for IPE sections in rural environment

$$\beta = \frac{\ln\left(\overline{R}/\overline{Q}\right)}{\sqrt{V_R^2 + V_Q^2}} \tag{31}$$

where, $\overline{R}$ and $\overline{Q}$ are the mean values of the resistance and load effects and V_R and V_Q are the coefficient of variations. The mean strength and the coefficient of variation (COV) of a compact beam are given in Eqs. (32) and (33).

$$\overline{R} = R_n\left(\lambda_M \lambda_P \lambda_F\right) \tag{32}$$

$$V_R = \sqrt{V_M^2 + V_P^2 + V_F^2} \tag{33}$$

where: λ_M, λ_P, and λ_F are material, professional, and geometry bias coefficients. The final bias factor for resistance λ_R is calculated as $\lambda_R = \lambda_M \lambda_P \lambda_F$. R_n is the nominal strength and can be described as $C_{b*}M_{ocr}$ in this study. Reliability indices were calculated by Galambos (2004), that result in $\lambda_R = 1.05$, $V_R = 0.1$ for a uniform moment and $\lambda_R = 1.23$, $V_R = 0.14$ for beams subjected to moment gradients, with a lognormal distribution. Detailed information for random variables for resistance and load are given in Table 5.

The nominal resistance R_n is determined using proposed method and have to be equal to load effect that is specified by ASCE 7–10. The load effect is determined using following Eqs. 34–35.

$$\overline{Q} = \overline{D} + \overline{L} \tag{34}$$

$$\sigma_Q^2 = D_n^2\left[(1.05 * 0.1)^2 + \left(\frac{L_n}{D_n} * 0.25\right)^2\right] \tag{35}$$

where: D_n is defined as nominal dead and L_n is defined as nominal live load for 50 year periods by Galambos et al. (1982). $\overline{D} = 1.05D_n, V_D = 0.1$ and $\overline{L} = L_n, V_L = 0.25$. Galambos (2004) assumed live load distribution as lognormal for ease of calculation. Therefore, live load is taken as a lognormal distribution in this study. Moreover, it can be said that the results are relatively affected by live load distribution (Eamon et al., 2017).

ASCE/SEI 7-10 (2010) specifies dead and live load factors of 1.2 and 1.6 for the combination of dead and live loads. In this study, the reliability is considered only load combination of $1.2DL + 1.6LL$ because Galambos (2004)

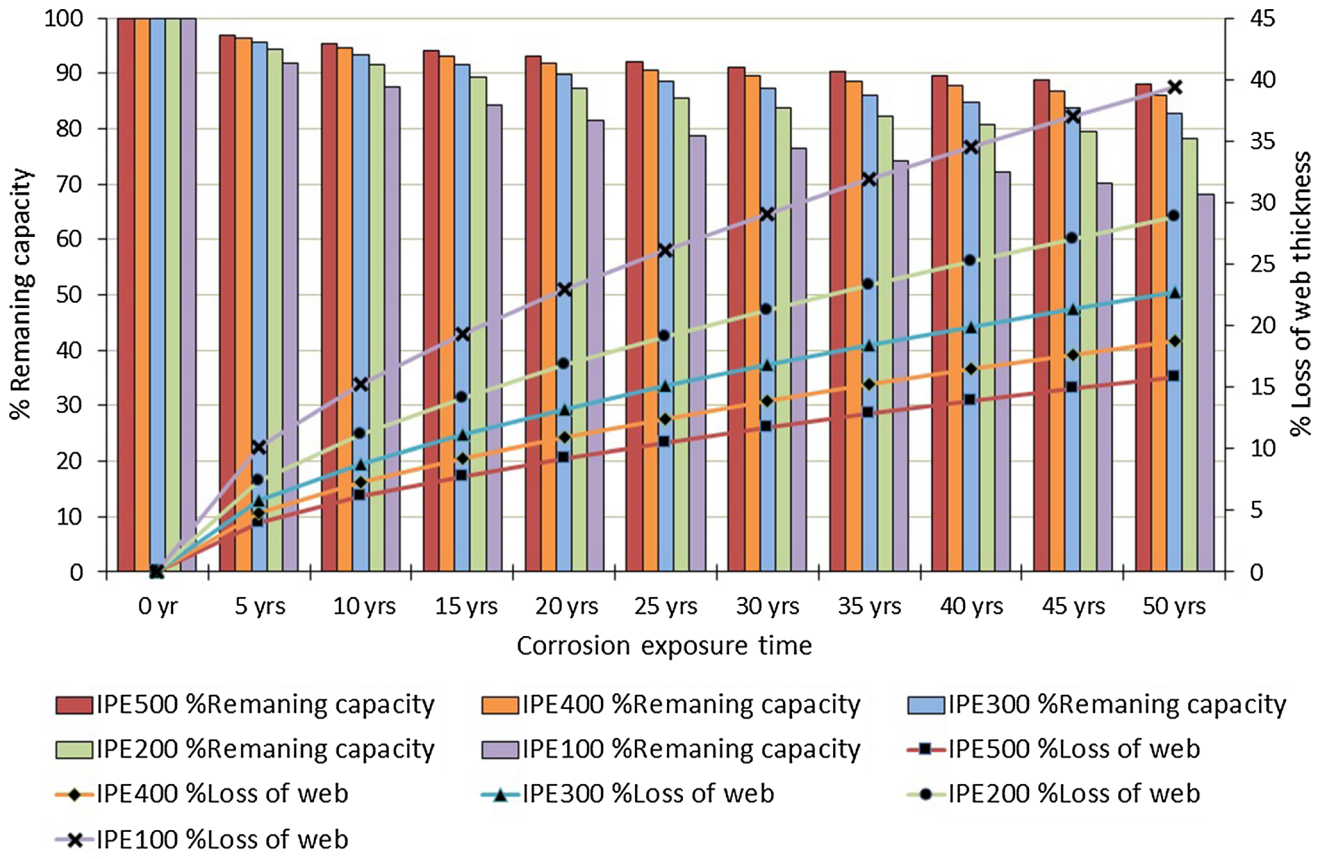

Fig. 13 % Remaining capacity versus % Loss of web thickness due to corrosion for IPE sections in urban environment

shows that this load combination gives the most critical reliability index values, β.In order to ensure safety of the member, Eq. (36) have to be satisfied.

$$\varphi R_n \geq 1.2D_n + 1.6L_n \tag{36}$$

In this study, First-Order Second-Moment (FOSM) reliability method is used to evaluate reliability index values. Besides, Monte Carlo Simulations (MCS) are used to verify the results. Reliability index values of FOSM and MCS are in good agreement.

AISC (LRFD) defines the target reliability index as 2.6 for a live to dead load ratio (L_n/D_n) of 3. Also, (Galambos, 2004) presented that the reasonable lower bound reliability index for these types of member is 2.6, when the discrimination error is not taken into account. Besides, White and Kim (2008) stated that the reliability index corresponds to 2.6 according to the ASCE 7 load model and elastic LTB.

In Fig. 20 reliability indices are calculated using the mentioned resistance statistics by Galambos (2004). The use of these values in Eq. (31) along with a resistance factor $\Phi = 0.9$ and an assumed live to dead load ratio (L_n/D_n) of 3 gives β equal to 2.6. As expected, this value is approximately same to the targeted reliability index defined in Galambos (2004). In addition, this figure gives information about LTB. In this case, analytical methods applied to determine the elastic LTB capacity are not applied. In this case, instead of the analytical methods used to determine the elastic LTB capacity, a fixed bias factor is used, as in the reliability studies previously mentioned in the study. In this way, conceptual reliability level in AISC (LRFD) is represented in Fig. 20.

In this study, effect of corrosion on the reliability of the steel members is investigated. Therefore, corrosion loss parameters A and B are mentioned in the previous section determined from the analyses of experimental data. These parameters are assumed lognormal variables. Therefore, the actual corrosion loss, C is also a random variable. In order to investigate corrosion effect on the steel members, mean (μ) and coefficient of variation (COV) values are given in Table 6.

Consequently, the limit state function for beam members subjected to LTB and corrosion can be expressed as follow.

$$Z(x) = M_{cr} - M_{DL} - M_{LL} \tag{37}$$

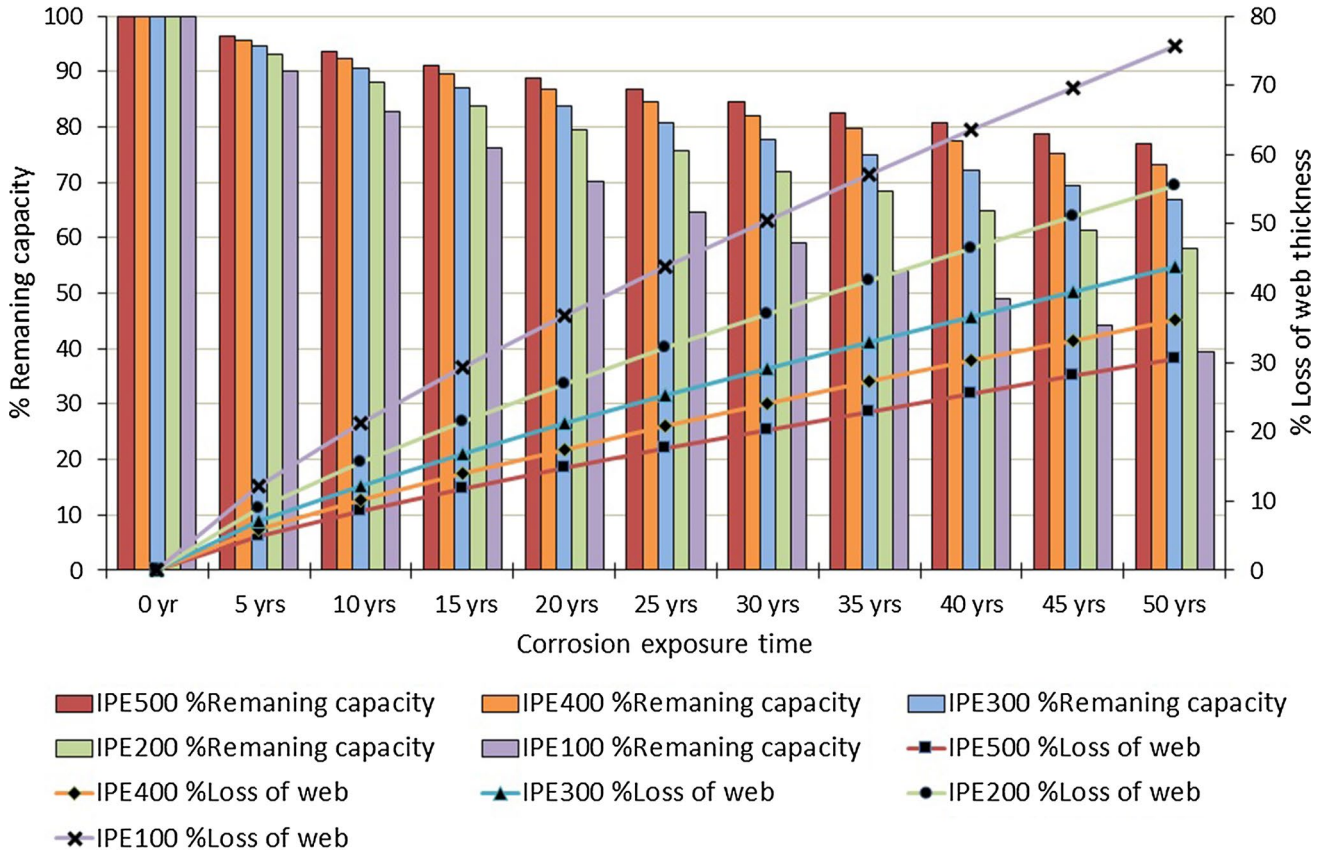

Fig. 14 % Remaining capacity versus % Loss of web thickness due to corrosion for IPE sections in marine environment

where: $Z(x)$ is the safety margin, M_{cr} is a random variable representing the resistance ultimate strength of member, M_{DL} and M_{LL} are random variables for dead and live loads.

M_{cr} can be estimated by an analytical procedure that includes section properties of section depend on thicknesses (J, polar moment of inertia, I_w, warping constant, and I_z, second moment of area about the minor axis), and C_b which is directly depend on end moment ratio (Ψ). M_{cr} can be described as

$$M_{cr} = M_{cr}\left(t, C_b\right) \tag{38}$$

In addition to these, the thickness values of the members at any specific time due to corrosion (depend on environment type) are expected to change. Therefore, A and B, which are the parameters of the corrosion rate, are also considered random variables.

Here, the obtained capacity ratios are similar for most beam sizes and spans exposed to elastic LTB, but capacity ratios are expected to differ depending on the effects of corrosion on cross sections.

In order to show research methodology of this study, a flowchart is generated and given in Fig. 21.

4.1 Reliability Analysis for End Moment Ratios, (Ψ)

The estimated reliability index, β values are obtained using the mentioned approaches. Graphic is plotted to illustrate β values for live to dead load ratio (L_n/D_n) of 3 and end moment ratios, Ψ of $-1 \le \Psi \le 1$. Results are plotted and given in Fig. 22.

Analyses results show that change in end moment ratios, Ψ effect significantly reliability of the member. This result is expected because the steel beams exposed to the linear moment gradient (change in Ψ) reduce or increase the strength. Moreover, different beam sizes (examined *IPE* sections in this study) and unbraced lengths (L_b = 8, 10, 12 and 16 m) exposed to elastic LTB are investigated and same reliability values are obtained from the analyses.

Moreover, formulation is created in order to calculate reliability index for I-beams subjected to elastic LTB and given in Eq. (39).

$$\beta(\Psi) = \frac{-0.2814\Psi^4 + 0.5076\Psi^3 + 2.776\Psi^2 - 3.249\Psi + 1.112}{\Psi^2 - 1.126\Psi + 0.3862} \tag{39}$$

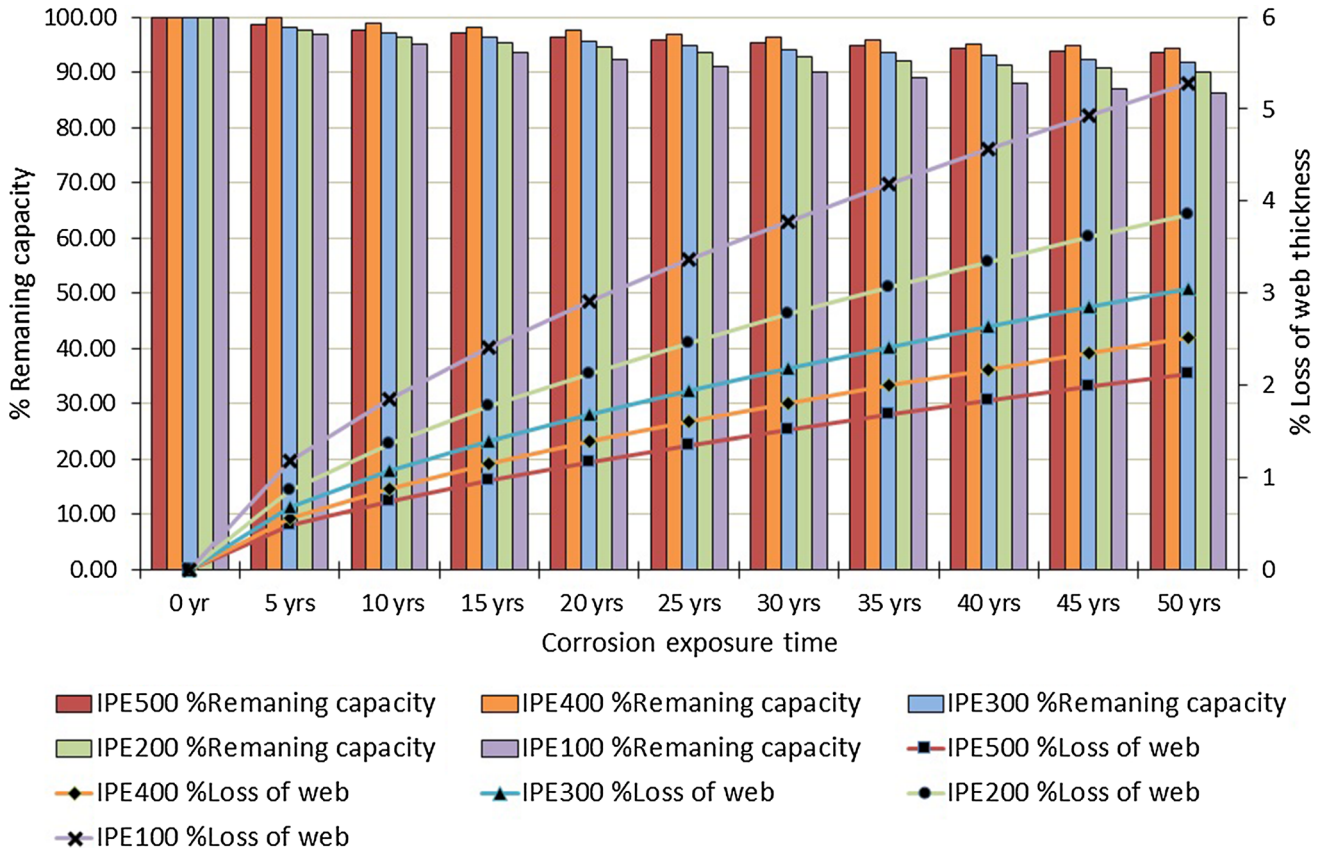

Fig. 15 % Remaining capacity versus % Loss of web thickness due to corrosion for IPE sections in rural environment

4.2 Reliability Analysis for Years of Corrosion Exposure and End Moment Ratio, ($\Psi = 1$)

Corrosion effects the members load carrying capacity depend on the environment and time. In addition, it is stated in the previous sections that the sections with different dimension properties are affected by corrosion differently. Section properties of the member (J, polar moment of inertia, I_w, warping constant, and I_z, second moment of area about the minor axis etc.) change differently depend on the corrosion exposure time and environment. Accordingly, it is expected that the reliability index values vary for each section. In order to show this changes, results are given in Figs. 23, 24, 25 for uniform thickness loss model and in Figs. 26, 27, 28 for varying thickness loss considering only one type of end moment ratio, ($\Psi = 1$) case and live to dead load ratio is assumed as $L_n/D_n = 3$.

According to the analyses results, safety level of all of the I-beams are effected dramatically by corrosion especially for beams, which have smaller cross section properties. In addition, it is seen that marine environment have a high damage affect compared other environments before reaching the 10 years.

4.3 Reliability Analysis for Years of Corrosion Exposure and End Moment Ratios, (Ψ)

The cross-section values of structural member are a function of two parameters, A and B that is used to calculate corrosion rate. Therefore, these parameters are assumed lognormal variables in the analyses. M_{cr} is estimated by an analytical calculation procedure, which includes the cross-sectional properties, modulus of elasticity, and end moment ratios. Consequently, the load carrying capacity (M_{cr}), load effects, and cross-section properties of the member are also assumed as random variables in the analyses.

Reliability analyses are performed to determine the safety of I-shaped steel members under the linear moment gradient by corrosion effect. Three types of environment condition are considered in here. Besides, end moment ratios for $-1 \leq \Psi \leq 1$ are taken into account in the analyses and live to dead load ratio is assumed as $L_n/D_n = 3$. Results are given in Figs. 29 and 30 for rural, urban and marine environment type and uniform and varying thickness loss models, respectively.

The parameters used to calculate resistance of the member are estimated and therefore they include uncertainty. When the values comes from created surfaces are examined

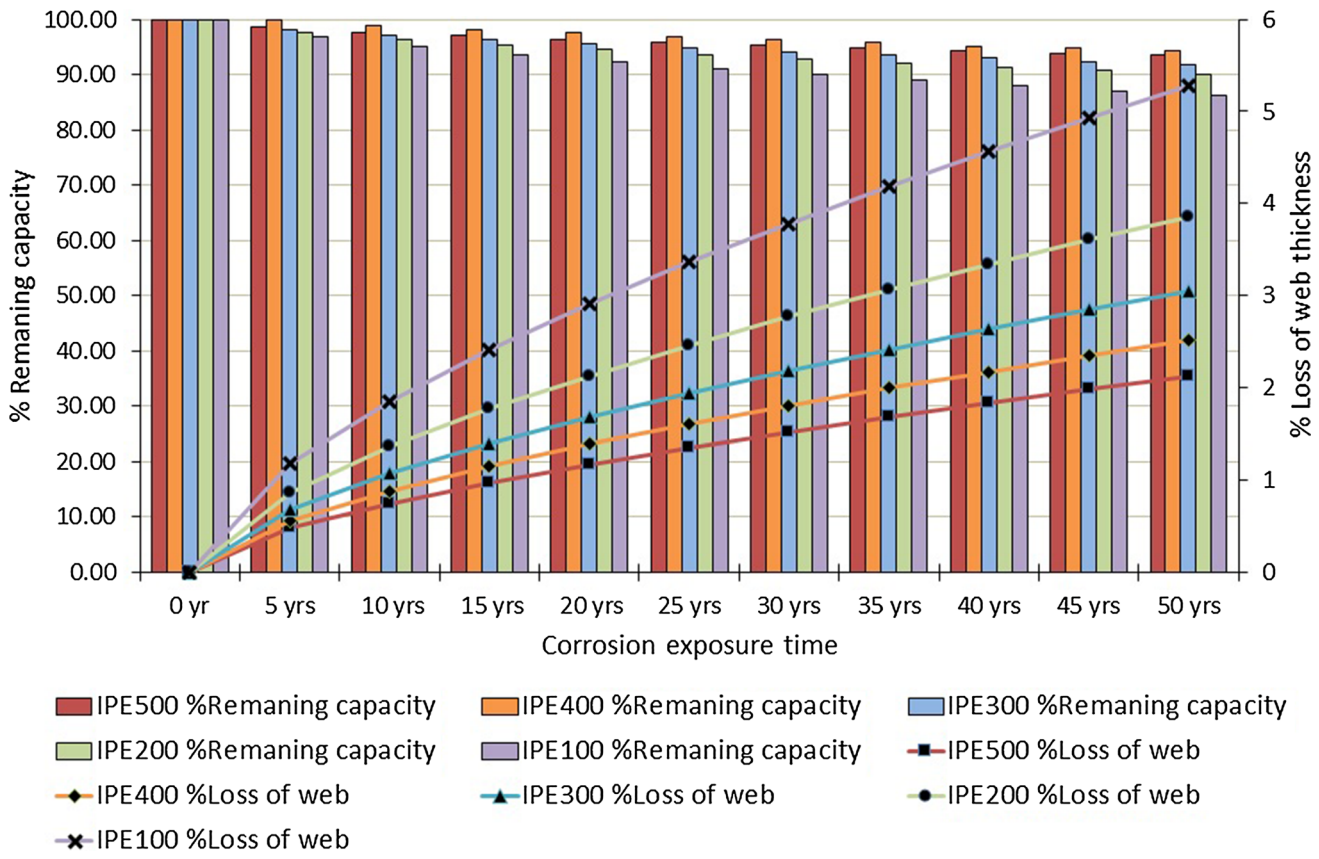

Fig. 16 % Remaining capacity versus % Loss of web thickness due to corrosion for IPE sections in urban environment

in detail for the 50-year period, it can be concluded that these parameters have an important effect on reliability of the member. Reliability index, β values are influenced significantly due to these parameters. However, here the most effective parameter appears to be B. A has a minor effect compared to B.

Corrosion models show that the rural environment has the most negligible effect on safety among three different environments. Moreover, end moment ratios also influence directly the safety of the member. Especially, range of $-1 \leq \Psi \leq 0$ has a negative effect on the reliability of the member.

Uniform corrosion cause the loss of material that results decreasing in the geometric properties of the member (cross sectional area, moment of inertia, section modulus, polar moment of inertia, warping constant, etc.). Thickness loss in the both the flanges and web of the member due to corrosion induce reduction in the moment capacity. Moreover, the stiffness of the members is expected to decline significantly and this may cause too many deflections in the member. In addition, uniform surface corrosion loss has an effect compression strength of the member due to buckling.

In here, it is not complicated to predict the probability of I-beams subjected to elastic LTB and corrosion for different environments. Therefore, formulations are created for all examined section depend on the applied end moment ratio and corrosion exposure time. Thus, instead of calculating the design values of I-beams, it is convenient to determine reliability indices of members. This helps the designer make quick structural decisions in the design process. The proposed formulation is given in Eq. 40.

$$\beta(\Psi, t) = a + b * \Psi + c * t + d * \Psi * t + e * t^2 \tag{40}$$

For all examined I-shape section and environment conditions, constants in the formulation are given in Table 7 uniform thickness loss model and in Table 8 varying thickness loss model.

5 Conclusions

In this study, elastic lateral torsional buckling behavior of doubly symmetric I-shaped steel members is investigated considering different approaches from codes and literature. A specific function that accounts for moment gradient and moment modification factor, C_b is proposed. Moreover, reliability analyses are performed in order to determine the

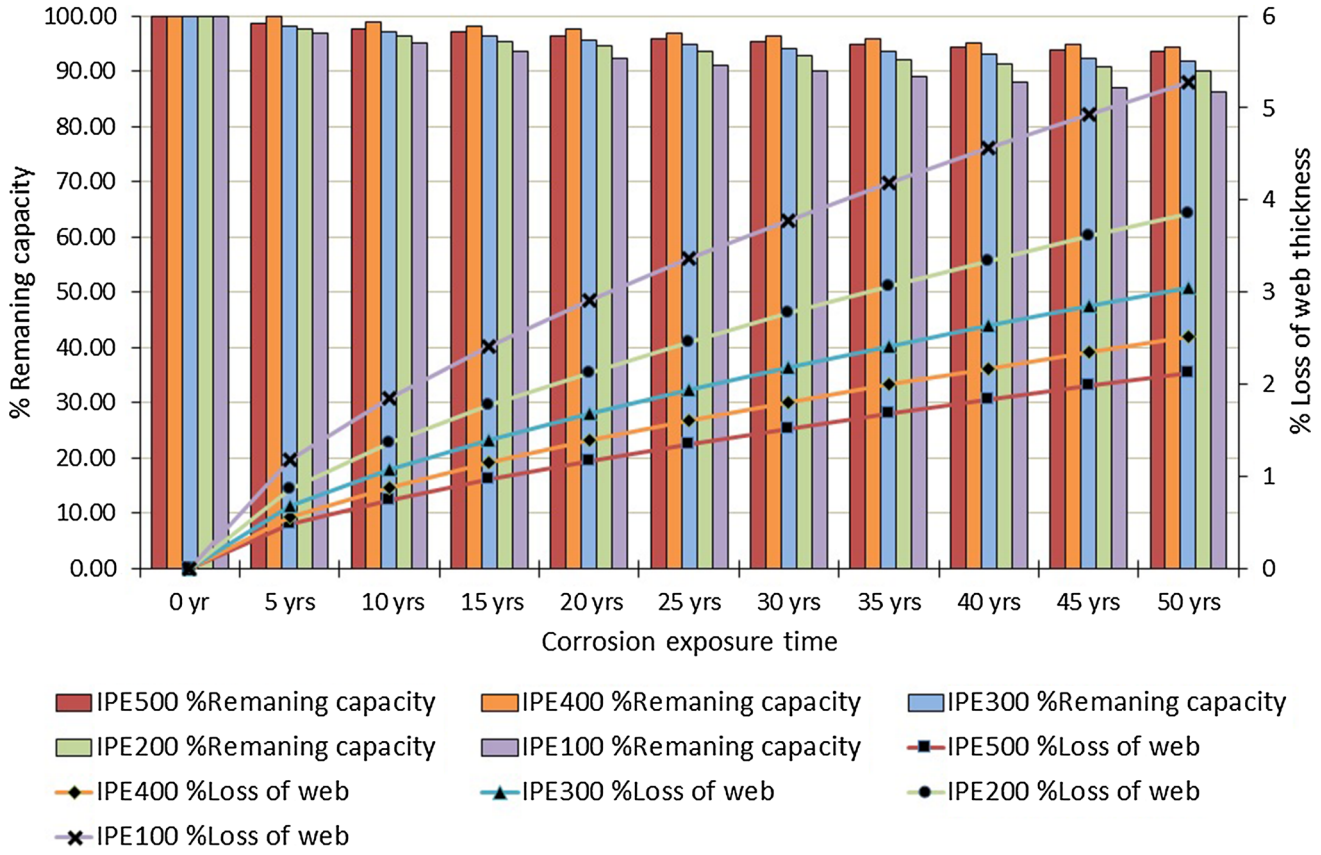

Fig. 17 % Remaining capacity versus % Loss of web thickness due to corrosion for IPE sections in marine environment

Table 3 Ultimate capacity decrease of IPE sections for different environments and uniform thickness loss model in 50 years' corrosion exposure

Section type	Environment		
	Rural	Urban	Marine
	% Capacity decrease at 50 years		
IPE500	6.87	13.61	29.88
IPE400	8.04	15.93	34.95
IPE300	9.94	19.68	43.15
IPE200	12.58	24.89	54.48
IPE100	18.33	36.17	78.79

Table 4 Ultimate capacity decrease of IPE sections for different environments and varying thickness loss model in 50 years corrosion exposure

Section type	Environment		
	Rural	Urban	Marine
	% Capacity decrease at 50 years		
IPE500	6.77	12.62	28.90
IPE400	6.88	13.55	30.50
IPE300	8.96	16.93	35.72
IPE200	10.63	20.62	43.14
IPE100	14.75	28.33	57.99

safety of the beam members by corrosion, as well. In this way, the conditions of the beams exposed to corrosion under the effect of lateral torsion buckling have been investigated.

Results from the proposed method is relatively closer to finite element analysis than any other approaches, especially code-based approaches. Moreover, analyses results show that the proposed method and generated moment modification factor expression, C_b can be practically used to express accurately the load carrying capacity of the member for examined cases in this study.

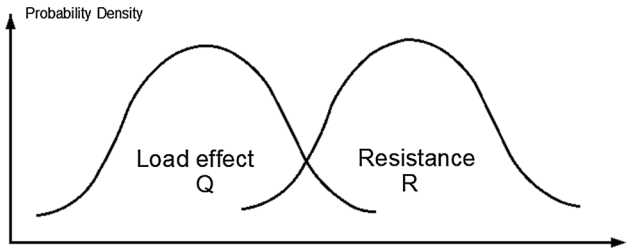

Fig. 18 Probabilistic description of resistance and load effect

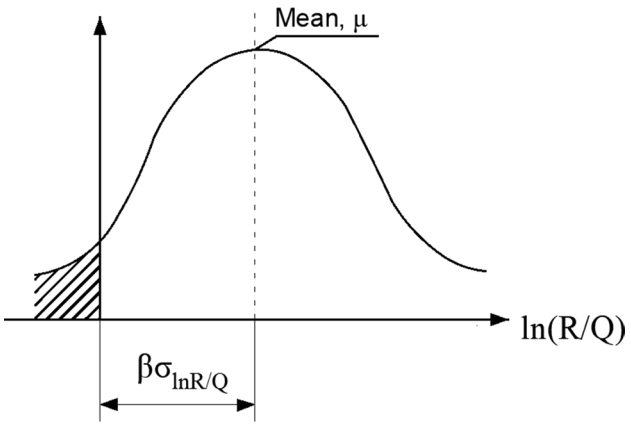

Fig. 19 Probabilistic description of resistance and load effect

Table 5 Random variables by Galambos (2004)

Random variable	Bias factor(λ)	COV	Distribution
Resistance			
Professional, *P*			
Uniform moment	0.99	0.06	Normal
Moment gradient	1.16	0.12	Normal
Elastic LTB	1.03	0.09	Normal
Fabrication, *F*	1.00	0.05	Normal
Material, *M*			
Yield	1.06	0.06	Normal
Elastic LTB	1.00	0.06	Normal
Uniform moment, M_{cr}	1.05	0.10	Lognormal
Derived resistance			
Moment gradient, M_{cr}	1.23	0.14	Lognormal
Elastic LTB	1.03	0.12	Lognormal
Load			
Dead load	1.05	0.10	Normal
Live load	1.00	0.25	Gumbel

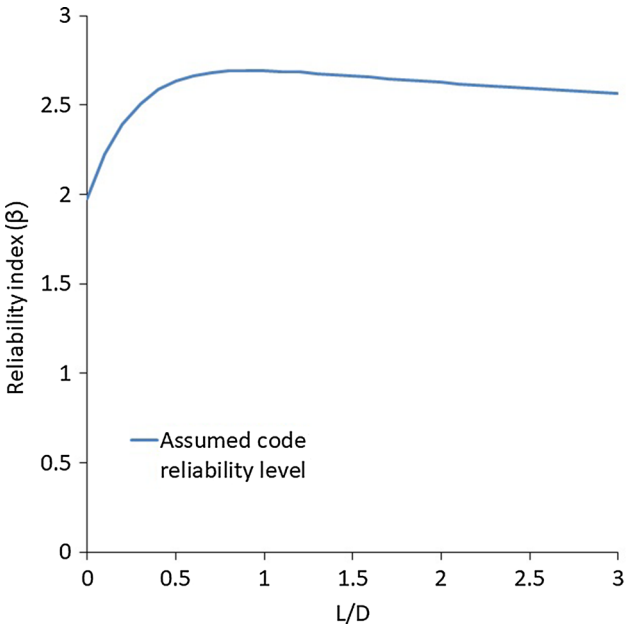

Fig. 20 Assumed code reliability level

Table 6 Random variables for *A* and *B* (Kayser & Nowak, 1989)

	Carbon Steel		Weathering Steel	
	A	B	A	B
Rural environment				
μ	34.0	0.65	33.3	0.5
COV	0.09	0.1	0.34	0.09
Urban environment				
μ	80.2	0.59	50.7	0.57
COV	0.42	0.4	0.30	0.37
Marine environment				
μ	70.6	0.79	40.2	0.56
COV	0.66	0.49	0.22	0.1

It is expected that elastic moment capacity of the beam subjected to lateral torsional buckling is decreased significantly by increases in the unbraced length, L_b. Furthermore, in order to decide exactly elastic moment a good estimation of the member under linear moment gradient depends on determination of moment modification factor, C_b.

According to the results of the analysis, the existing design code procedures used to determine the LTB capacity directly depend on the moment modification factor but far from demonstrating the actual strength of the elements. Therefore, this provides room for improvement in determining reliability of the member subjected to elastic LTB.

Corrosion models for examined steel beams are considered for years of corrosion exposure and three different environments as well. It is observed that the corroded steel beams have significantly drop in their reliability depending on the corrosion exposure time. Especially, capacity decreasing in the sections reaches very high levels for uniform section loss model. Their reliability level equally effected compared to varying thickness loss model. In this point, it has to be known that actual corrosion damage is local and not uniform and corrosion model should be selected reaching the more realistic solution.

According to analysis results, it can be concluded that the structural steel elements need to be repaired or renewed under the prescribed corrosion model within a certain time and depending on the environment in which they are located or precautions against corrosion should be taken rigorously. These cases will also constitute the future subject of the study.

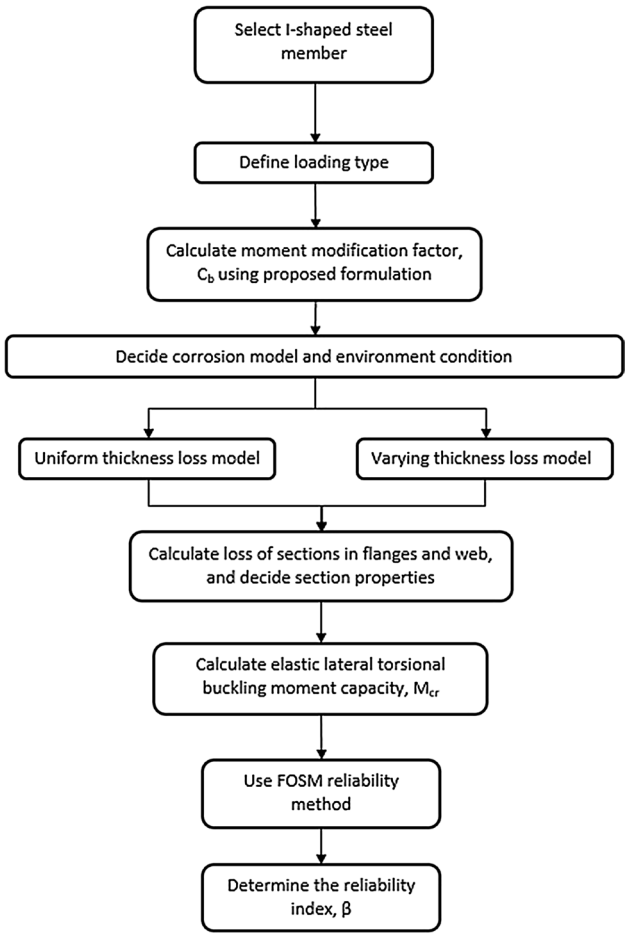

Fig. 21 A flow chart for research methodology

Consequently, identified corrosion models of the steel beams are investigated from different perspective. Formulations are generated in order to determine safety level of these beams depend on the corrosion exposure time and environment. It is presented that there are significant changes in the capacity that occur on a single beam element in the study. Therefore, more detailed structural investigations are recommended. However, it is believed that obtained analysis results and assessments will help designers and structure engineers to develop maintenance plans that would allow to keep safety at an acceptable level at low cost against coupled LTB and corrosion threat.

Fig. 22 Reliability index for end moment ratios and $L_n/D_n = 3$

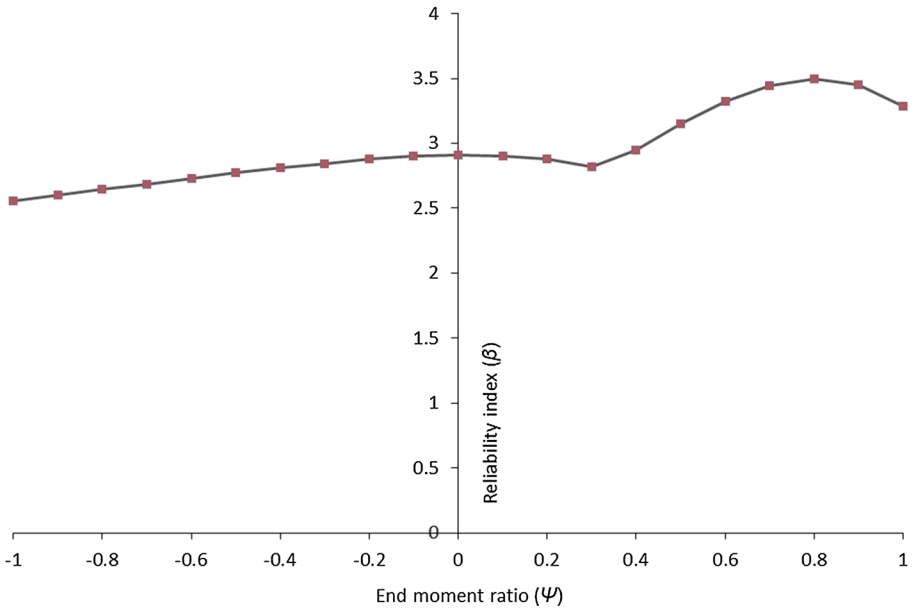

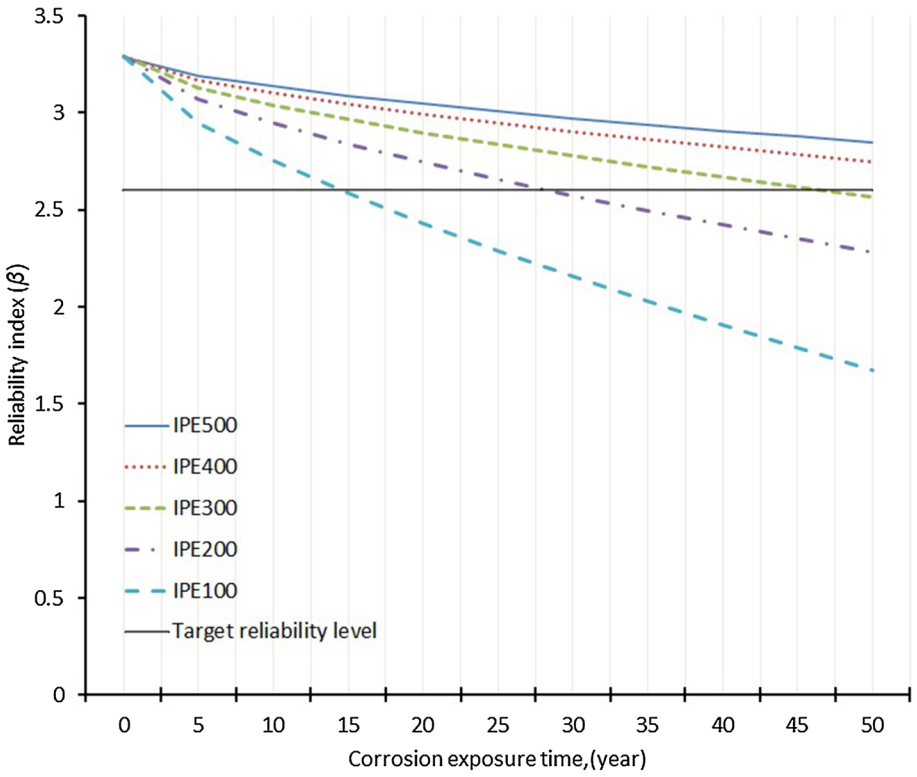

Fig. 23 Reliability index for end moment ratio $\Psi = 1$ versus years of corrosion exposure (uniform thickness loss) for rural environment

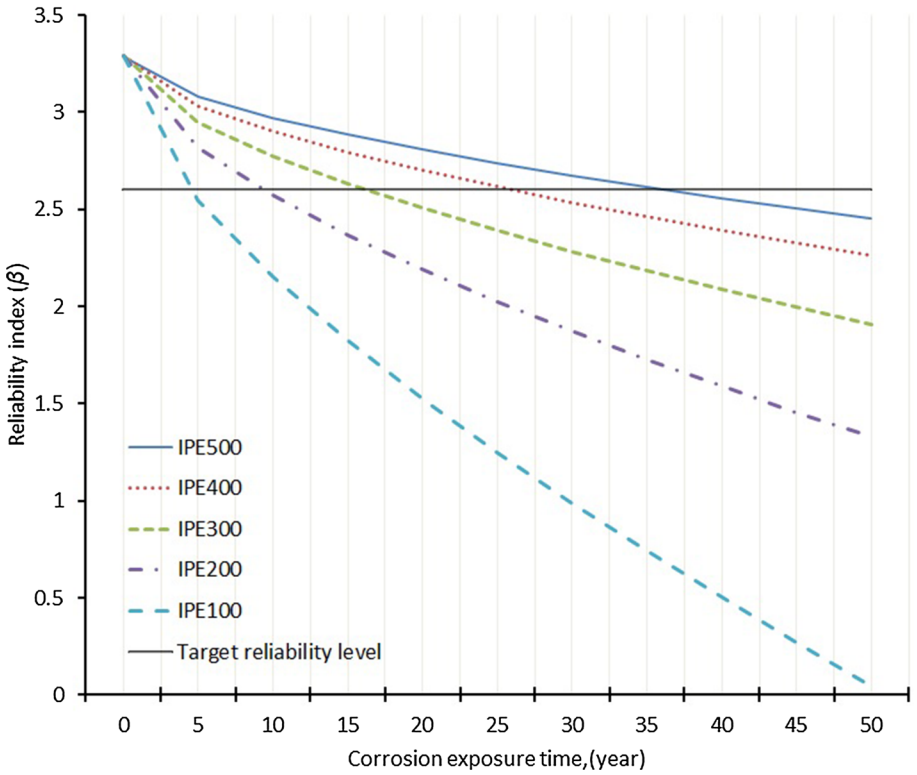

Fig. 24 Reliability index for end moment ratio $\Psi = 1$ versus years of corrosion exposure (uniform thickness loss) for urban environment

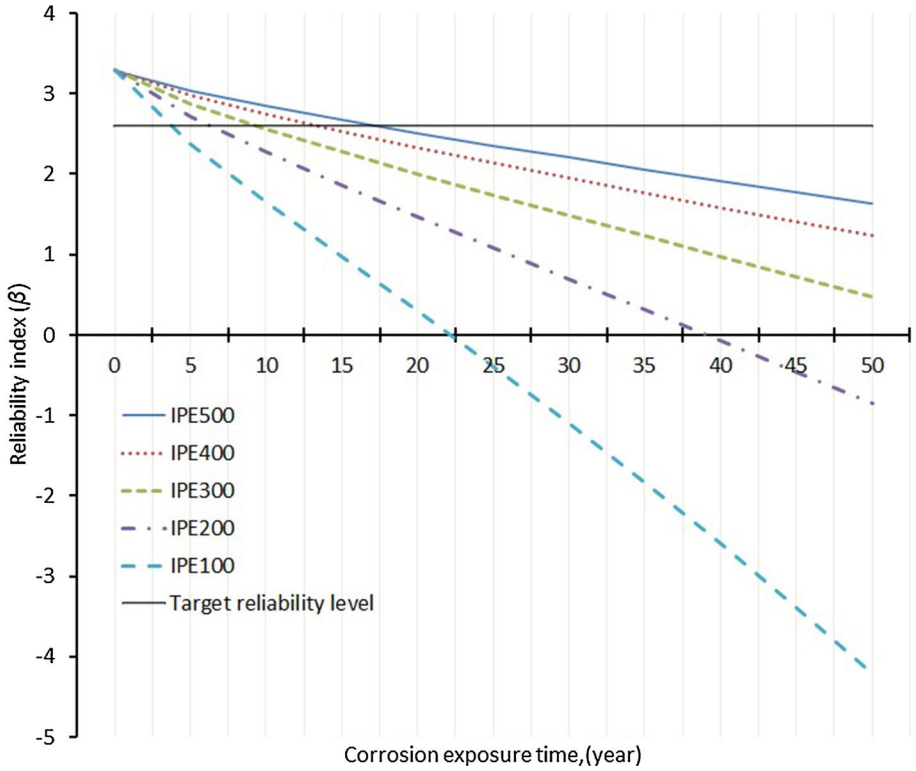

Fig. 25 Reliability index for end moment ratio $\Psi = 1$ versus years of corrosion exposure (uniform thickness loss) for marine environment

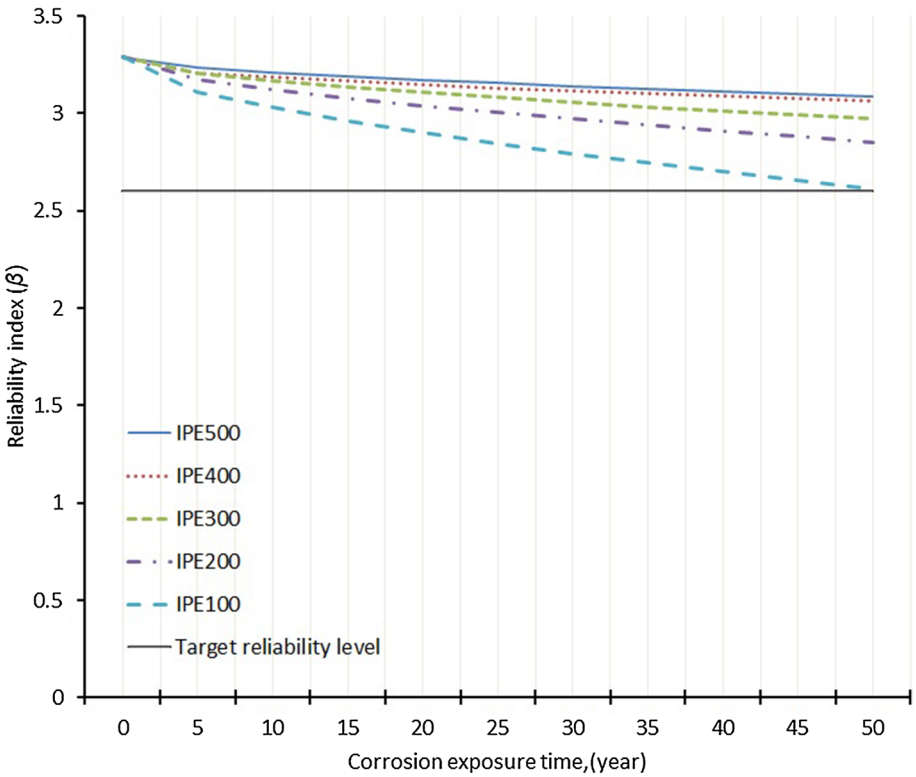

Fig. 26 Reliability index for end moment ratio $\Psi = 1$ versus years of corrosion exposure (varying thickness loss) for rural environment

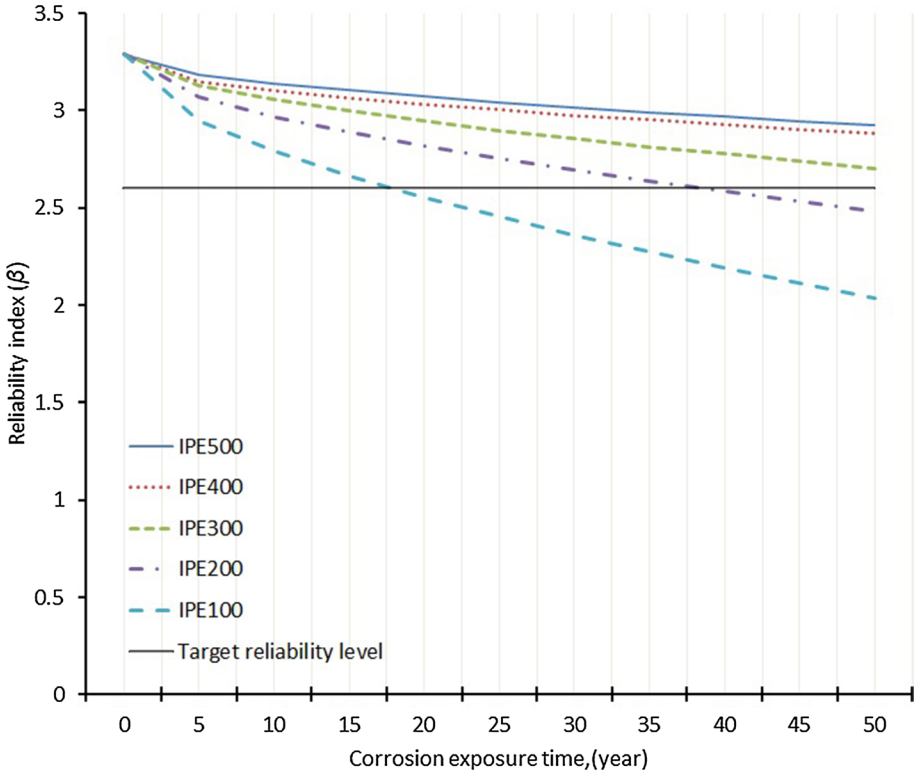

Fig. 27 Reliability index for end moment ratio $\Psi = 1$ versus years of corrosion exposure (varying thickness loss) for urban environment

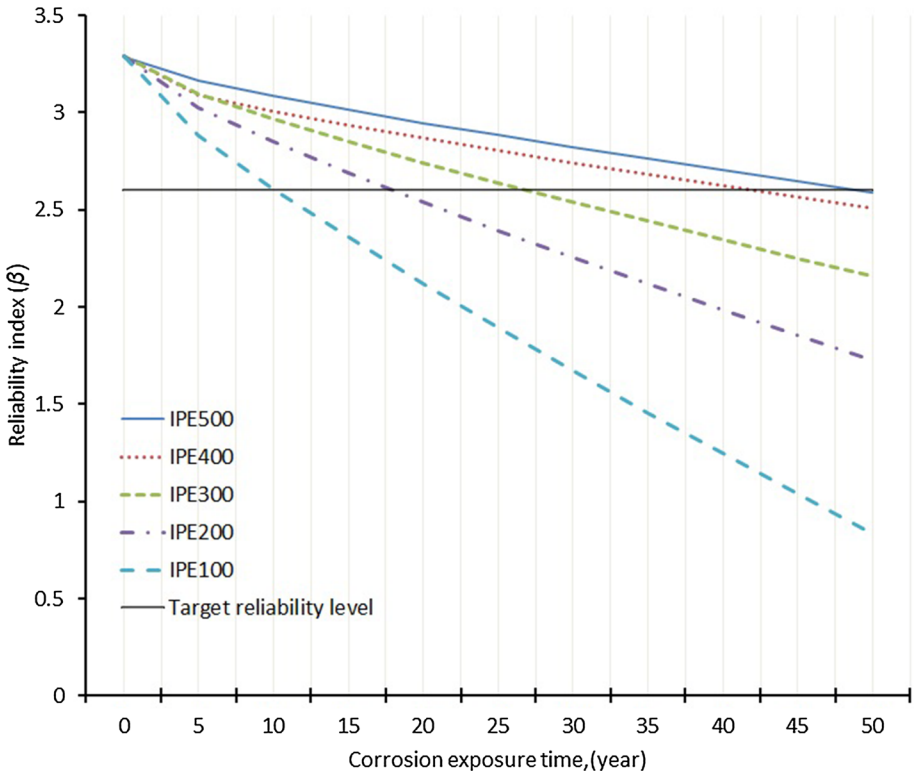

Fig. 28 Reliability index for end moment ratio $\Psi = 1$ versus years of corrosion exposure (varying thickness loss) for marine environment

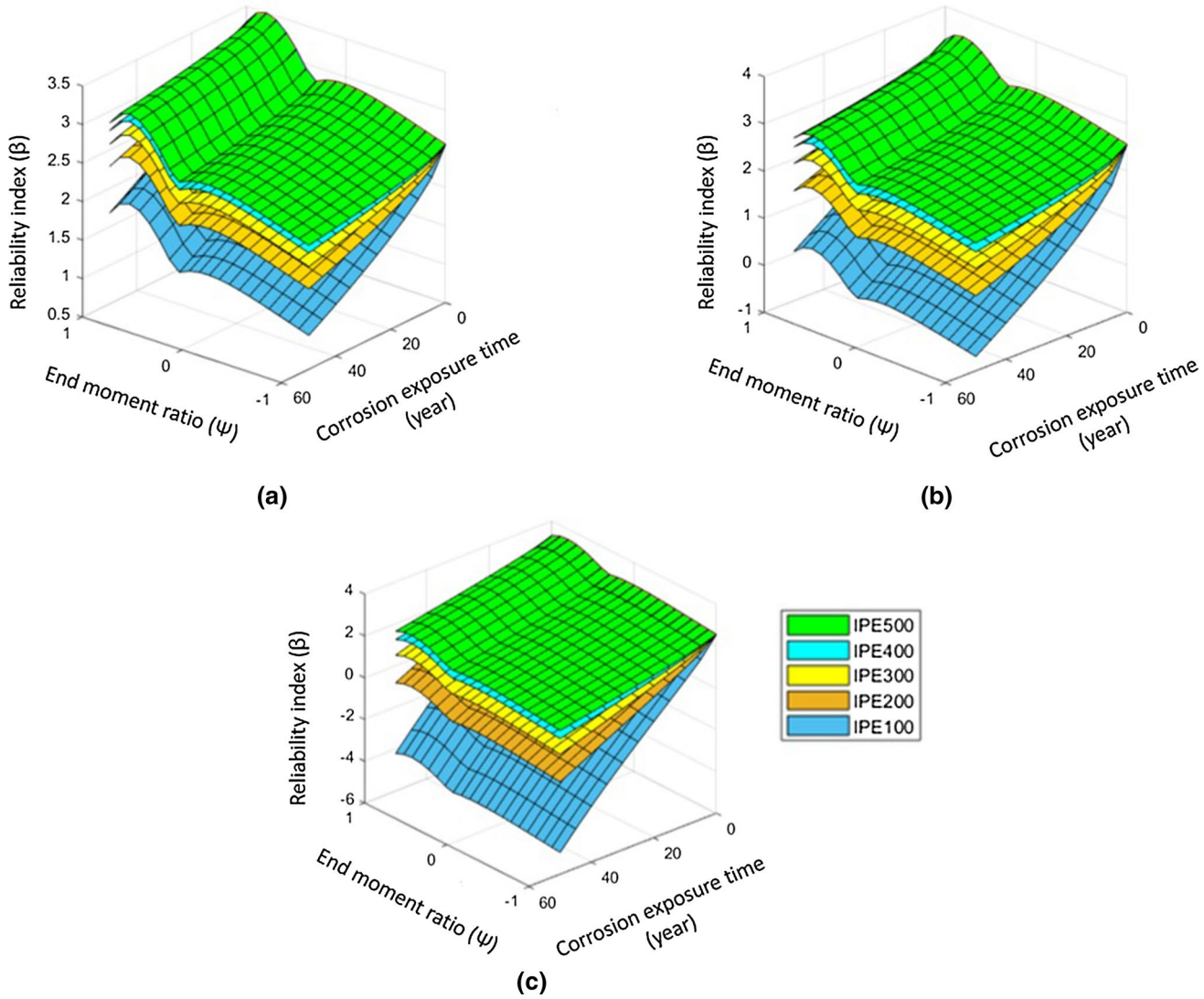

Fig. 29 Reliability index for end moment ratios versus years of corrosion exposure time for **a** rural **b** urban **c** marine environment

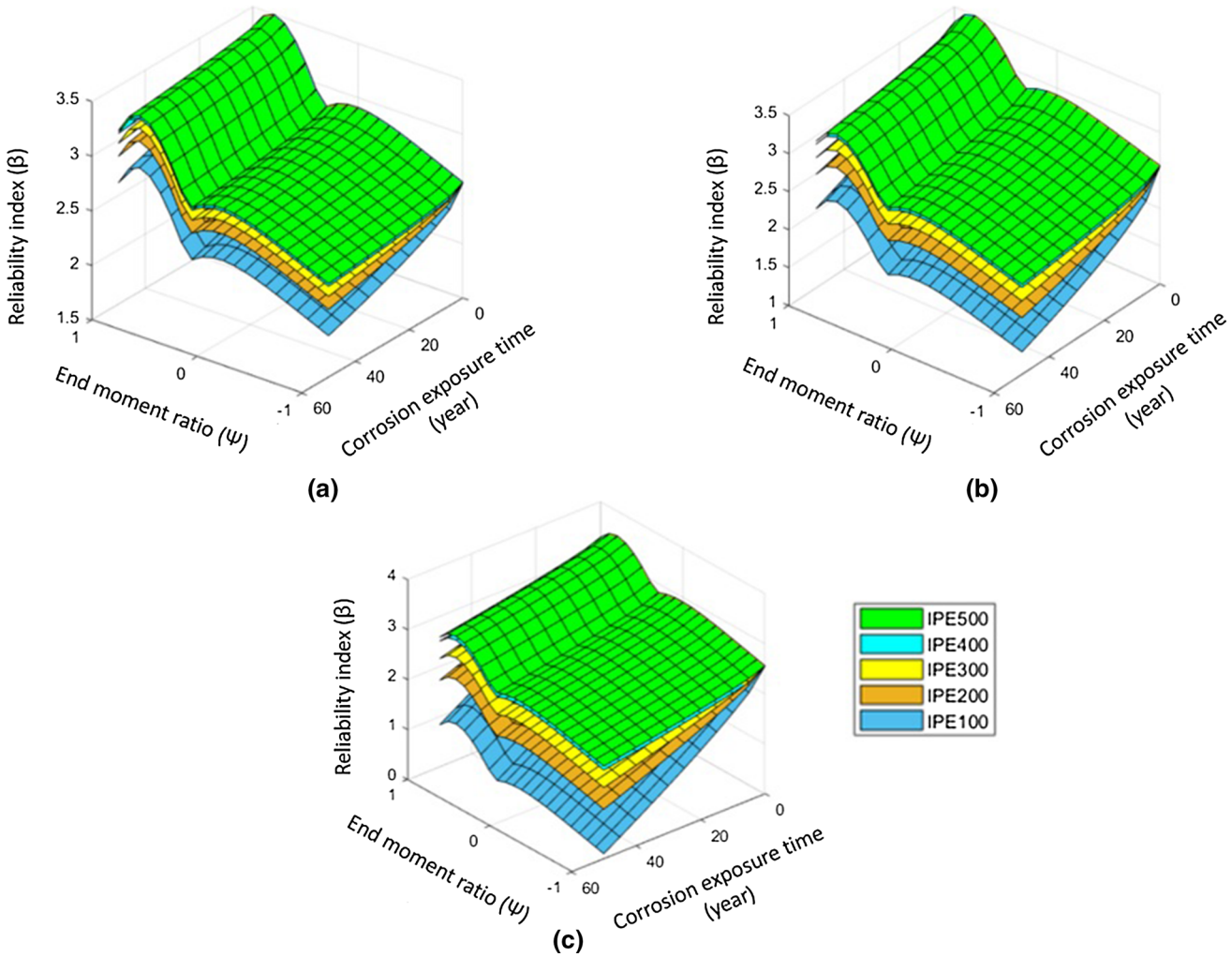

Fig. 30 Reliability index for end moment ratios versus years of corrosion exposure time for **a** rural **b** urban **c** marine environment

Table 7 Constant values for uniform thickness loss model in Eq. (40)

IPE section	Constants				
	a	b	c	d	e
Rural					
IPE500	2.925	0.4005	−0.01169	−0.00014	0.00007
IPE400	2.893	0.3393	−0.01586	−0.00006	0.00011
IPE300	2.900	0.4085	−0.01851	−0.00036	0.00011
IPE200	2.877	0.4119	−0.02571	−0.00039	0.00015
IPE100	2.893	0.4233	−0.04548	0.00051	0.00031
Urban					
IPE500	2.871	0.4175	−0.02224	−0.00054	0.00015
IPE400	2.860	0.4289	−0.02773	−0.00092	0.00019
IPE300	2.881	0.4224	−0.04158	0.00048	0.00033
IPE200	2.807	0.4819	−0.05331	−0.00207	0.00035
IPE100	2.674	0.4900	−0.08153	−0.00277	0.00045
Marine					
IPE500	2.900	0.4059	−0.03845	−0.00028	0.00013
IPE400	2.894	0.4142	−0.04752	−0.00049	0.00016
IPE300	2.866	0.4175	−0.06238	−0.00078	0.00016
IPE200	2.846	0.4426	−0.08728	−0.00141	0.00014
IPE100	2.781	0.4866	−0.13490	−0.00276	−0.00022

Table 8 Constant values for varying thickness loss model in Eq. (40)

IPE section	Constants				
	a	b	c	d	e
Rural					
IPE500	2.938	0.3988	−0.00552	−0.00011	0.00004
IPE400	2.933	0.4393	−0.00719	−0.00001	0.00007
IPE300	2.937	0.4392	−0.00951	−0.00002	0.00008
IPE200	2.930	0.4393	−0.01308	−0.00003	0.00010
IPE100	2.915	0.4393	−0.02042	0.00005	0.00016
Urban					
IPE500	2.931	0.4393	−0.01147	0.00003	0.00009
IPE400	2.915	0.4393	−0.01331	0.00003	0.00013
IPE300	2.918	0.4393	−0.01829	0.00005	0.00016
IPE200	2.904	0.4393	−0.02527	0.00007	0.00022
IPE100	2.879	0.4193	−0.03977	0.00014	0.00034
Marine					
IPE500	2.938	0.4392	−0.01786	0.00006	0.00009
IPE400	2.907	0.4393	−0.02165	0.00007	0.00015
IPE300	2.930	0.4391	−0.02864	0.00011	0.00014
IPE200	2.921	0.4389	−0.03960	0.00019	0.00019
IPE100	2.909	0.4381	−0.06295	0.00045	0.00032

References

AISC 360-16. (2016). *ANSI / AISC 360-16, Specification for structural steel buildings*. American Institute of Steel Construction, Chicago, Illinois, USA.

Albrecht, P., & Hall, T. T. (2003). Atmospheric corrosion resistance of structural steels. *Journal of Materials in Civil Engineering, 15*, 2–24.

ANSYS. (2015). Version 15.0, Canonsburg, Ansys. Inc.

AS4100 (1998). *Steel structures*. Standards Australia. Standards Association of Australia, Sydney, Australia

ASCE/SEI 7-10. (2010). *Minimum design loads for buildings and other structures*. Virginia, USA.

Aydin, M. R. (2009). Elastic flexural and lateral torsional buckling analysis of frames using finite elements. *KSCE Journal of Civil Engineering, 14*, 25–31.

BS5950. (2000). *Structural use of steelwork in building*. British Standards Institution, London, UK.

Chandrasekaran, S. (2019). *Advanced steel design of structures, 1 st edition.* CRC Press, Florida.

Chandrasekaran, S., & Jain, A. (2017). *Ocean structures: Construction, Materials and Operations*. CRC Press, Florida.

Chandrasekaran, S., & Nagavinothini, R. (2020). *Offshore compliant platforms: Analysis, design and experimental studies*. Wiley, UK.

CSA-S16 (2014). Design of steel structures. CSA standard S16–14. Mississauga: Canadian Standards Association.

Eamon, C. D., Lamb, A. W., & Patki, K. (2017). Effect of moment gradient and load height with respect to centroid on the reliability of wide flange steel beams subject to elastic lateral torsional buckling. *Engineering Structures, 150*, 656–664.

Ellingwood, B. E., Galambos, T. V., MacGregor, J. G., and Cornell, C. A. (1980). *Development of a probability based load criterion for American National Standard A58*. Washington, DC.

EN 1993-1-1 (1992). *Design of steel structures-Part 1–1: General rules and rules for buildings*. European Committee for Standardization, Brussel, Belgium.

Fontana, M. G. (1987). *Corrosion engineering, 3rd ed*. McGraw-Hill, Singapore.

Galambos, T. V. (2004). Reliability of the member stability criteria in the 2005 AISC specification. *Engineering Journal, American Institute of Steel Construction, 43*, 257–266.

Galambos, T. V., Ellingwood, B. E., MacGregor, J. G., & Cornell, C. A. (1982). Probability-based load criteria: Assessment of current design practice. *Journal of Structural Division, 108*, 959–977.

Ghafoori, E., & Motavalli, M. (2015). Lateral-torsional buckling of steel I-beams retrofitted by bonded and un-bonded CFRP laminates with different pre-stress levels: Experimental and numerical study. *Construction and Building Materials, 76*, 194–206.

Jankowska-Sandberg, J., & Kołodziej, J. (2013). Experimental study of steel truss lateral-torsional buckling. *Engineering Structures, 46*, 165–172.

Kayser, J. R., & Nowak, A. S. (1989). Capacity loss due to corrosion in steel-girder bridges. *Journal of Structural Engineering, 115*, 1525–1537.

Kirby, P. A., & Nethercot, D. A. (1979). *Design for structural stability*. Halsted Press, New York.

Komp, M. E. (1987). Atmospheric corrosion ratings of weathering steels—calculation and significance. *Materials Performance, 26*, 42–44.

Kucukler, M., Gardner, L., & Macorini, L. (2015). Lateral-torsional buckling assessment of steel beams through a stiffness reduction method. *Journal of Constructional Steel Research, 109*, 87–100.

MATLAB. (2018). *Version R2018a*, Massachusetts, MATLAB Release. Natick.

Melchers, R. E. (1999). Corrosion uncertainty modelling for steel structures. *Journal of Constructional Steel Research, 52*, 3–19.

Melchers, R. E. (2003a). Probabilistic model for marine corrosion of steel for structural reliability assessment. *Journal of Structural Engineering, 129*, 1484–1493.

Melchers, R. E. (2003b). Probabilistic models for corrosion in structural reliability assessment—Part 1: Empirical models. *Journal of Offshore Mechanics and Arctic Engineering, 125*, 264–271.

Ozbasaran, H., Aydin, R., & Dogan, M. (2015). An alternative design procedure for lateral—torsional buckling of cantilever I-beams. *Thin Walled Structures, 90*, 235–242.

Rahgozar, R. (2009). Remaining capacity assessment of corrosion damaged beams using minimum curves. *Journal of Constructional Steel Research, 65*, 299–307.

Rahgozar, R., Sharifi, Y., & Malekinejad, M. (2010). Buckling capacity of uniformly corroded steel members in terms of exposure time. *Steel and Composite Structures, 10*, 475–487.

Rahgozar, R. (1998). Fatigue endurance of steel structures subjected to corrosion. Ph.D. thesis, The University of Bristol.

Salvadory, M. (1955). Lateral buckling of I-beams. *ASCE Transaction, 120*, 1165–1177.

Saydam, D., & Frangopol, D. M. (2011). Time-dependent performance indicators of damaged bridge superstructures. *Engineering Structures, 33*, 2458–2471.

Serna, M. A., López, A., Puente, I., & Yong, D. J. (2006). Equivalent uniform moment factors for lateral-torsional buckling of steel members. *Journal of Constructional Steel Research, 62*, 566–580.

Sharif, Y., & Rahgozar, R. (2010). Remaining moment capacity of corroded steel beams. *International Journal of Steel Structures, 10*, 165–176.

Sharifi, Y., & Rahgozar, R. (2009). Fatigue notch factor in steel bridges due to corrosion. *Archives of Civil and Mechanical Engineering, 9*, 75–83.

Sharifi, Y., & Rahgozar, R. (2010a). Simple assessment method to estimate the remaining moment capacity of corroded I-beam sections. *Scientia Iranica, 17*, 161–167.

Sharifi, Y., & Rahgozar, R. (2010b). Evaluation of the remaining shear capacity in corroded steel I-beams. *Advanced Steel Construction, 6*, 803–816.

Sharifi, Y., & Rahgozar, R. (2010c). Evaluation of the remaining lateral torsional buckling capacity in corroded steel members. *Journal of Zhejiang University: Science A, 11*, 887–897.

Sharifi, Y., & Tohidi, S. (2014). Lateral-torsional buckling capacity assessment of web opening steel girders by artificial neural networks—elastic investigation. *Frontiers of Structural and Civil Engineering, 8*, 167–177.

Timoshenko, S. P., & Gere, J. (1985). *Theory of elastic stability, 2nd ed*. McGraw-Hill, New York.

TSDC-2016. (2016). *Turkish steel design code*. Ministry of Environment and Urbanization, Ankara, Turkey.

Uzun, E. T., & Seçer, M. (2019). Lateral torsional buckling of doubly symmetric I-shaped steel members under linear moment gradient. *Pamukkale University Journal of Engineering Sciences, 25*(6), 635–642.

Valarinho, L., Correia, J. R., Machado-e-Costa, M., Branco, F. A., & Silvestre, N. (2016). Lateral-torsional buckling behaviour of long-span laminated glass beams: Analytical, experimental and numerical study. *Materials and Design, 102*, 264–275.

White, D. W., & Kim, Y. D. (2008). Unified flexural resistance equations for stability design of steel I-section members: Moment gradient tests. *Journal of Structural Engineering, 134*, 1450–1470.

Winkler, R., Kindmann, R., & Knobloch, M. (2017). Lateral torsional buckling behaviour of steel beams: On the influence of the structural system. *Structures, 11*, 178–188.

Wong, E., & Driver, R. G. (2010). Critical evaluation of equivalent moment factor procedures for laterally unsupported beams. *ASCI Engineering Journal, 47*, 1–20.

Wu, L., & Mohareb, M. (2013). Finite-element formulation for the lateral torsional buckling of plane frames. *Journal of Engineering Mechanics, 139*, 512–524.

Yang, B., Kang, S.-B., Xiong, G., Shidong, N., Hu, Y., Wang, S., Bai, J., & Dai, G. (2017). Experimental and numerical study on lateral-torsional buckling of singly symmetric Q460GJ steel I-shaped beams. *Thin-Walled Structures, 113*, 205–2016.